Nonlinear Dynamics and Chaos

Prof. George Haller
Transcription: Trevor Winstral

2022

Contents

Chapter 1

Introduction

First we shall introduce the most important characters in our following exploration. The ideas and definitions here will be recurring regularly as we examine them from different perspectives and using different tools. The content covered by this course can be found in the following books. For further details on some of the results, we recommend consulting these.

- J. Guckenheimer & P. Holmes, Nonlinear Oscillations, Dynamical Systems and Bifurcations of Vector Fields,
- F. Verhulst, Nonlinear Differential Equations and Dynamical Systems,
- V. I. Arnold, Ordinary Differential Equations,
- S. Strogatz, Nonlinear Dynamics and Chaos.

Definition 1.1 (Dynamical System (DS))**.** A triple $(P, E, \mathcal{F})$, with

- P : the phase space for the dynamical variable $x \in P$,
- E : base space of the evolutionary variable (e.g. time) $t \in E$,
- $\mathcal{F}$: the evolution rule (deterministic) which defines the transition from one state to the next.

The two main types of evolutionary variable spaces are

(i) Discrete dynamical systems (DDS) $t \in E = \mathbb{Z}$ with trajectory $\{x_0, x_1, \ldots\}$,

(ii) Continuous dynamical systems (CDS) $t \in E = \mathbb{R}$ with trajectory $\{x_t\}_{t\in\mathbb{R}}$.

Corresponding to these there are various types of evolution rules

(i) In a DDS we have iterated mappings

$$\boxed{x_{n+1} = F(x_n, n).}$$

If there is no explicit dependence on n, i.e. $\frac{\partial F}{\partial n} = 0$, then

$$\boxed{x_{n+1}F(x_n) = F(F(x_{n-1})) = \underbrace{F \circ \ldots \circ F}_{n+1 \text{ times}}(x_0) = F^{n+1}(x_0).}$$

Example 1.1 (Cobweb diagram of a one-dimensional DDSs). In such cases and in one-dimensional problems, a simple way to analyze the behavior of the system is the so-called *cobweb* diagram. We may plot x_{n+1} as a function of x_n, as demonstrated in Fig. 1.1. The image of an initial condition x_0 lies on the graph at $x_{n+1} = F(x_0)$. We can also compute the next iterate by horizontally projecting the point $(x_0, F(x_0))$ to the diagonal line defined by $x_{n+1} = x_n$. Following the porjection of this point to the horizontal axis (x_n) we find the intersection with the graph at the point $(x_1, F(x_1))$. It follows that fixed points on the cobweb diagram correspond to the intersection of the graph of F with the diagonal line $x_{n+1} = x_n$.

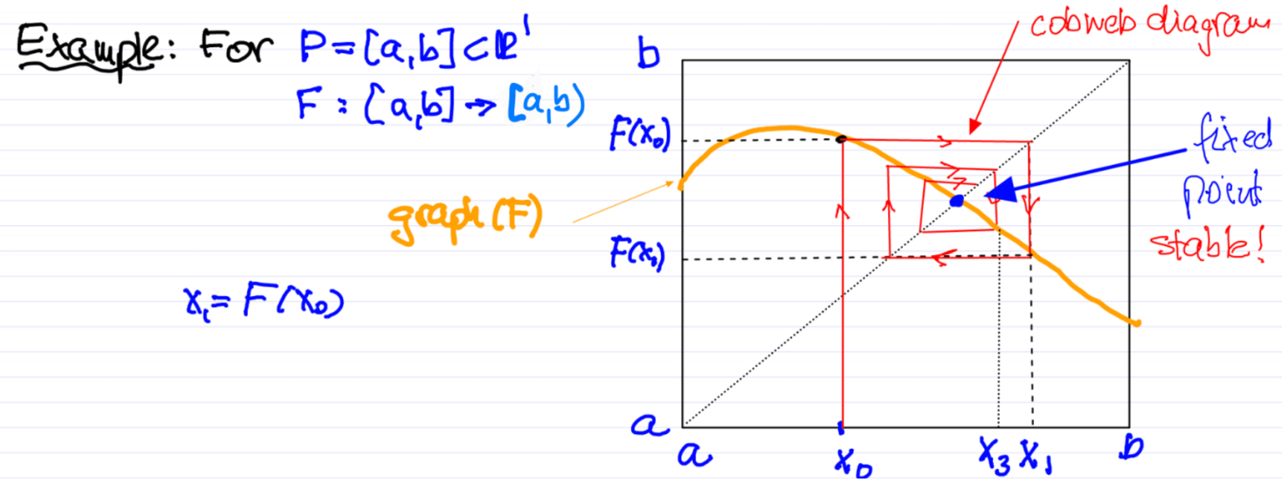

Figure 1.1: Analysis of a one-dimensional system defined on the interval $x \in [a, b]$ using the cobweb diagram

(ii) In a CDS we have a first order system of ordinary differential equations (ODE)

$$\boxed{\dot{x} = f(x, t)}$$

for $x \in P$ and $t \in E$. This yields the initial value problem (IVP):

$$\begin{cases} \dot{x} = f(x,t) \\ x(t_0) = x_0 \end{cases}$$

Assuming there exists a unique solution $\varphi(t;t_0,x_0)$ with $\dot{\varphi} = f(\phi,t)$ and $\varphi(t_0) = x_0$, then the following flow map is well defined

$$\boxed{F_{t_0}^t(x_0) := \varphi(t;t_0,x_0).}$$

Geometrically, this solution can be viewed as a trajectory in phase space (cf. Fig. 1.2).

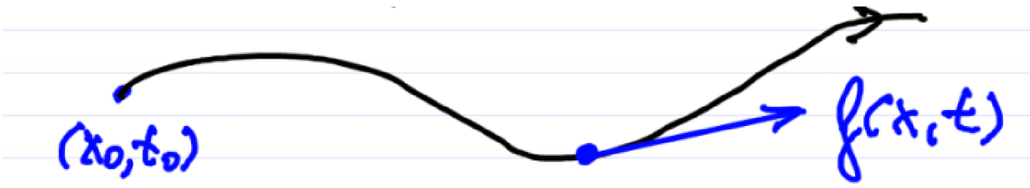

Figure 1.2: Trajectory of a continuous dynamical system. The RHS is given by f(x,t), which is the tangent vector to this curve at the point x at time t.

Such an $F_{t_0}^t$ has the properties

(a) $F_{t_0}^t$ is as smooth as $f(x,t)$,

(b) $F_{t_0}^{t_0} = I$ and $F_{t_0}^{t_2} = F_{t_1}^{t_2} \circ F_{t_0}^{t_1}$,

(c) $\left(F_{t_0}^t\right)^{-1} = F_t^{t_0}$ exists and is smooth.

Properties (a) and (b) together are called the group property. A special case of continuous dynamical systems is the autonomous system.

$$\boxed{\dot{x} = f(x).}$$

The autonomy of a system implies

$$x(s,t_0,x_0) = x(\underbrace{s-t_0}_{t},0,x_0) \stackrel{!}{=} x(t,x_0).$$

The induced flow map in this case is the one-parameter family of maps

$$\boxed{F^t = F_0^t : x_0 \mapsto x(t,x_0).}$$

Example 1.2 (Logisitic Equation). For a resource-limited population, we have the following dynamical system for $a > 0$, $b > 0$, and the population $x \in \mathbb{R}_+ \cup \{0\}$

$$\dot{x} = ax(b - x).$$

In this case we have $E = \mathbb{R}$ and $\mathcal{F} = \{F^t\}_{t=-\infty}^{+\infty}$. This system has globally existing unique solutions (see later). We may analyze the behavior of this system by plotting $\dot{x}$ as a function of x, analogously to the cobweb diagram. This is demonstrated in Fig. 1.3. At x values, where $\dot{x}$ is positive $x(t)$ is growing, while at negative values it is decreasing. This means, that fixed points, at which $x(t) = \text{const.}$ correspond to intersections of the graphs with the horizontal axis.

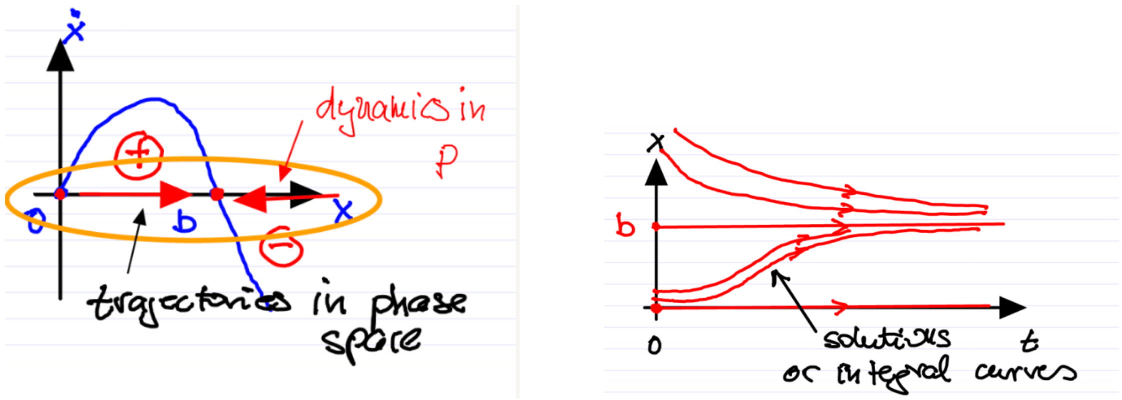

Figure 1.3: Left: Analysis of the right hand side. Right: Evolution in the extended phase space $P \times \mathbb{R}$.

Example 1.3 (Pendulum). Given the equation of motion

$$ml^2\ddot{\varphi} = -mgl\sin(\varphi).$$

We let $x_1 = \varphi$ and $x_2 = \dot{\varphi}$ to transform into the first-order ODE form

$$\begin{cases} \dot{x}_1 = x_2 \\ \dot{x}_2 = -\dfrac{g}{l}\sin(x_1). \end{cases}$$

Thus we have

$$x = \begin{pmatrix} x_1 \\ x_2 \end{pmatrix}; \quad f(x) = \begin{pmatrix} x_2 \\ -\frac{g}{l}\sin(x_1) \end{pmatrix}.$$

Qualitative analysis gives the following facts

- $(x_1, x_2) = (0, 0)$ and $(x_1, x_2) = (\pi, 0)$ are zeros of f.
- Energy is conserved, hence both small and large amplitude oscillations are expected.
- The function $f(x)$ has symmetries: it is invariant under the transformation $(x_1, x_2, t) \mapsto (x_1, -x_2, -t)$ and $(x_1, x_2, t) \mapsto (-x_1, x_2, -t)$. See the left panel of Fig. 1.4.

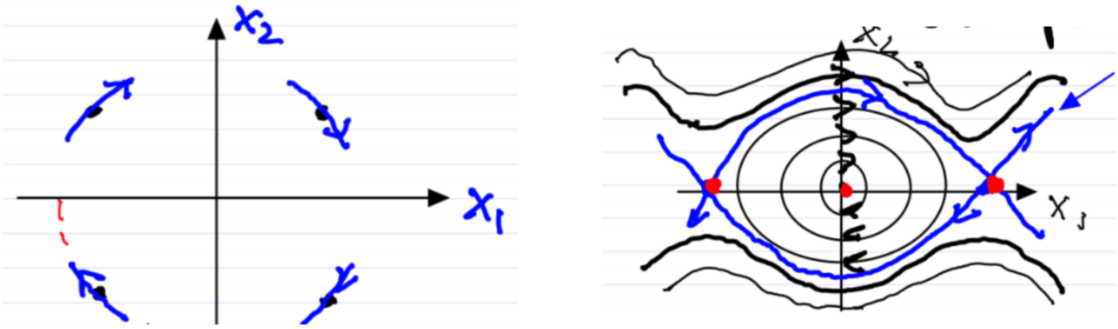

Figure 1.4: Left: The symmetries of the dynamical system. Right: Phase portrait of the pendulum. Red dots show the fixed points, while the blue trajectories make up the separatrix.

Definition 1.2. A separatrix is a boundary (i.e. a codimension-1 surface) in phase space which separates regions of qualitatively different behaviors. In practice, it is unobservable by itself and connects different fixed points. The separatrix of the pendulum is shown in the right panel of Fig. 4.

Example 1.4 (Exploit geometry of phase space for analysis)*.* Consider two cities, A and B. The two cities are connected by two roads, denoted by the blue and green curves of the left panel of Fig. 1.5. We assume that travelling on the two roads, it is possible for two bikes to make it from A to B without ever being further away from each other than a distance $d < D$.

Assume two trucks are trying to make it between A and B, on different roads in the opposite direction, carrying a load of width D. Given this information, can the trucks make it without hitting each other? We can view this problem as a continuous dynamical system with two coordinates x_1 and x_2 that parameterize the two routes between A and B. This dynamical system is, in general, non autonomous.

The right panel of Fig 1.5 shows the trajectories of the two trucks and the two bikes in phase space. The two trajectories must intersect by continuity, thus at that point the trucks must be at the same positions as the bikes, implying they are within distance D. Therefore the trucks must crash!

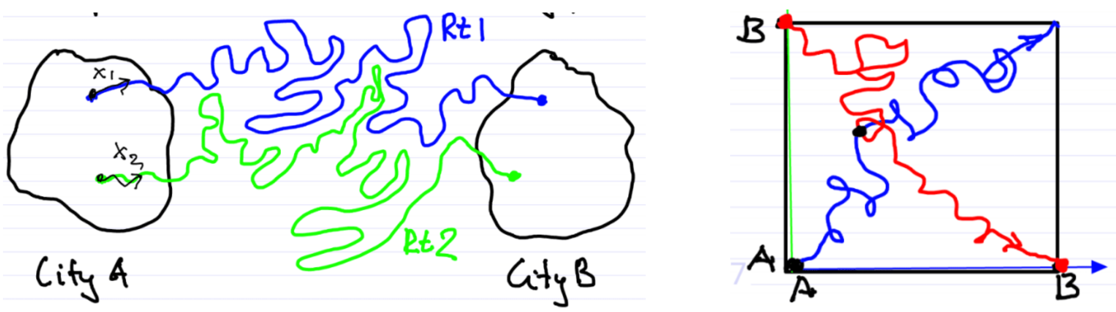

Figure 1.5: Left: An example of the two bike routes. Right: Blue represents the trajectory of the two bikes, red represents the trajectory of the two trucks.

Chapter 2

Fundamentals

In this chapter, we first review some fundamental properties of continuous dynamical systems that will be used heavily in later chapters. As we will see, these technical results are interesting in their own right. They can help in interpreting or cross-checking numerical results or physical models for self-consistency or accuracy.

2.1 Existence and uniqueness of solutions

Consider

$$\begin{cases} \dot{x} = f(x,t); \quad x \in \mathbb{R}^n \\ x(t_0) = x_0 \end{cases}.$$

Does this initial value problem have a unique solution? We have the following theorems to help us answer that question.

Theorem 2.1 (Peano). *If $f \in C^0$ near (x_0, t_0), then there exists a local solution $\varphi(t)$, i.e.,*

$$\dot{\varphi}(t) = f(\varphi(t), t), \varphi(t_0) = x_0; \ \forall t \in (t_0 - \epsilon, t_0 + \epsilon); \ 0 < \epsilon \ll 1.$$

Example 2.1 (Free falling mass). Consider a point mass of mass m at position x. The acceleration due to gravity is denoted by g. Measuring the potential energy from the reference point $x = x_0$, we have the total energy is conserved.

$$\frac{1}{2} m \dot{x}^2 = mg(x - x_0).$$

This implies that

$$\begin{cases} \dot{x} = \sqrt{2g(x - x_0)} \\ x(0) = x_0 \end{cases}$$

on the set $P = \{x \in \mathbb{R} : \ x \geq x_0\}$. Therefore we have that $f \in C^0$ in phase space, so by Peano's theorem (cf. Theorem 2.1), there exists a local solution. A schematic diagram is shown in Fig. 2.1. The solution is actually $x(t) = x_0 + \frac{g}{2}(t - t_0)^2$, however $x(t) = x_0$ is also a solution to

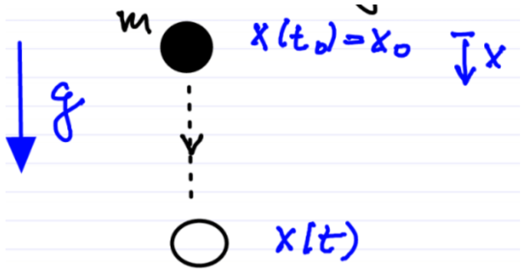

Figure 2.1: Schematic diagram of the point mass in free fall.

the IVP, therefore we do not have a unique solution. Physically there exists a solution, but this IVP was derived from a heuristic energy-principle, not from Newton's laws, which are not equivalent.

Definition 2.1. A function f is called locally Lipschitz around x_0 if there exists an open set U_{x_0} and $L > 0$ such that for all $x, y \in U_{x_0}$

$$\boxed{\|f(y,t) - f(x,t)\| \leq L\|y - x\|.}$$

Example 2.2 (Lipschitz functions)*.* Fig. 2.2 shows an example of a Lipschitz and a non-Lipschitz function around x_0.

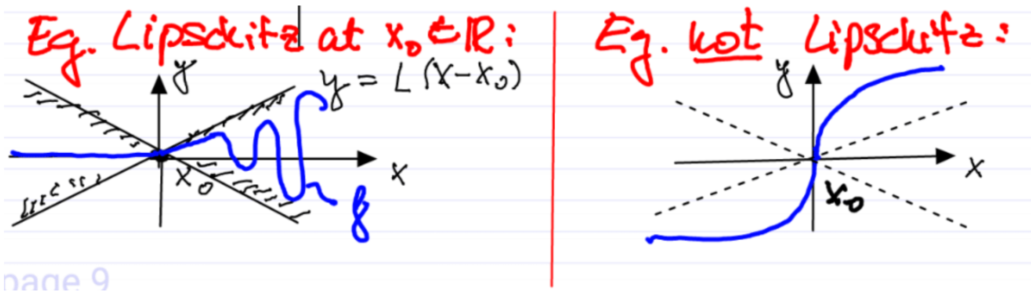

Figure 2.2: Interpretation of the Lipschitz property.

Theorem 2.2 (Picard)**.** *Assume*

(i) $f \in C^0$ *in* t *near* (t_0, x_0),

(ii) f *is locally Lipschitz in* x *near* (t_0, x_0).

Then there exists a unique local solution to the IVP. The proof can be found in Arnold's book on ODEs.

Note the following relations. If f is $C^1 \implies f$ is Lipschitz $\implies f$ is C^0.

Example 2.3 (Free falling mass revisted). We check if f is Lipschitz.

$$\frac{|f(x) - f(x_0)|}{|x - x_0|} = \frac{\sqrt{2g}}{\sqrt{|x - x_0|}} \geq L|x - x_0|.$$

Thus f is not Lipschitz near x_0.

2.2 Geometric consequences of uniqueness

If the solution is unique, we have a few facts that can be derived from the geometric point of view.

(i) The trajectories of autonomous systems cannot intersect. Note that fixed points do not violate this (e.g. pendulum equations). See Fig. 2.3 which shows the phase portrait of the pendulum.

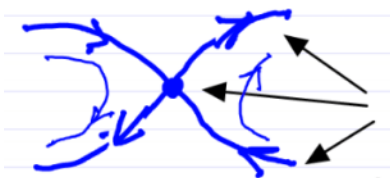

Figure 2.3: The phase portrait of the pendulum. Trajectories do not intersect since each arrow is pointing at separate trajectories.

(ii) For non-autonomous systems, intersections in phase space are possible: a trajectory may occupy the same point x at a different time instants (see the left panel of Fig. 2.4. In this case we can extend the phase space in order to get an autonomous system where there cannot be any intersections.

$$X = \begin{pmatrix} x \\ t \end{pmatrix}, \; F(X) = \begin{pmatrix} f(x,t) \\ 1 \end{pmatrix}; \; \dot{X} = F(X).$$

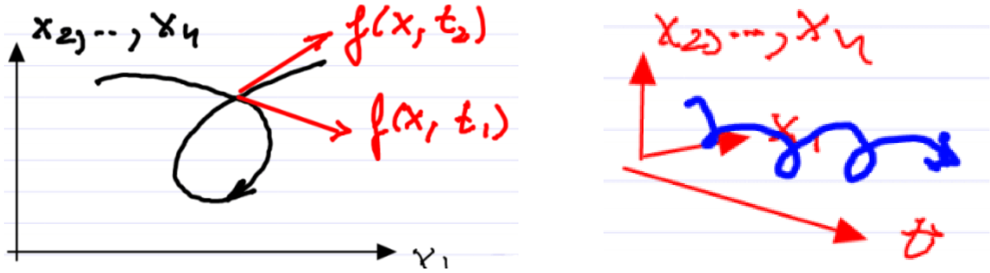

Figure 2.4: Left: Intersecting trajectories in phase space for a non-autonomous system. Right: The same trajectory in the extended phase space, without intersections.

2.3 Local vs global existence

Example 2.4 (Exploding solution).

$$\begin{cases} \dot{x} = x^2 \\ x(t_0) = 1. \end{cases}$$

Integrating yields the solution $x(t) = \frac{1}{1-(t-t_0)}$. This solution blows up at $t_\infty = t_0 + 1$, therefore the solution is only local. This is demonstrated in Fig. 2.5.

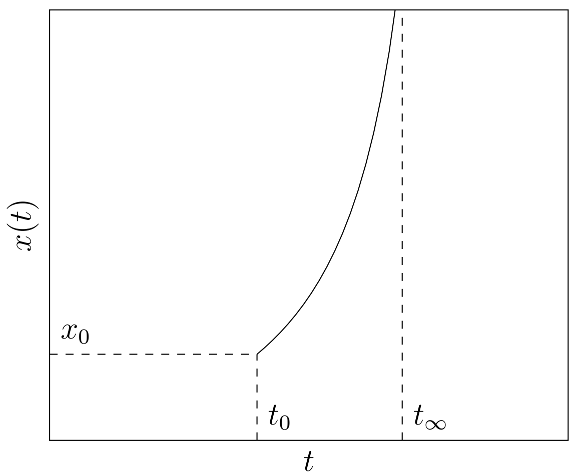

Figure 2.5: Solution to the ODE $\dot{x} = x^2$ started from $x(t_0) = 1$.

To address this problem of local solutions not being able to be continued into global solution, we have the following theorem.

Theorem 2.3 (Continuation of solution). *If a local solutions cannot be continued to a time $t = T$, then we must have*

$$\boxed{\lim_{t \to T} \|x(t)\| = \infty.}$$

The proof can be found in Arnold's book on ODEs.

Example 2.5 (Coupled Pendulum System). Consider two pendula of masses m_1 and m_2. They both have length l. The angles of these pendula are denoted by φ_1 and φ_2. Let us assume that they are coupled by a nonlinear spring, which can be described by a potential $V(\varphi_1, \varphi_2)$. This setup is illustrated in Fig. 2.6. We set $x_1 = \varphi_1,\ x_2 = \dot{\varphi}_1,\ x_3 = \varphi_2,\ x_4 = \dot{\varphi}_2$ and get the following equation of motion

$$\begin{cases} \dot{x}_1 = x_2 \\ \dot{x}_2 = \dots \\ \dot{x}_3 = x_4 \\ \dot{x}_4 = \dots \end{cases}$$

The RHS is smooth, therefore there exists a unique local solution to any IVP. The phase space

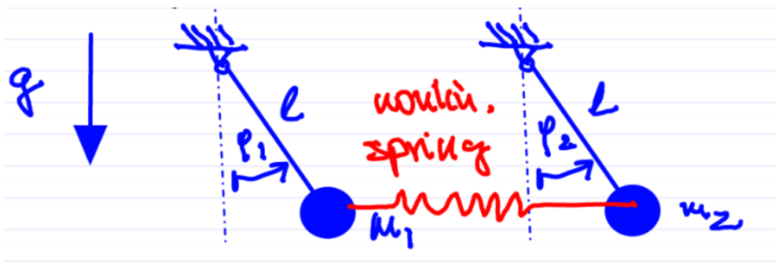

Figure 2.6: Physical setup of the coupled pendulum with a nonlinear spring.

is given by

$$P = \{x :\ x_1 \in S^1,\ x_2 \in \mathbb{R},\ x_3 \in S^1,\ x_4 \in \mathbb{R}\} = S^1 \times \mathbb{R} \times S^1 \times \mathbb{R}.$$

Where S^1 is the 1 dimensional sphere (i.e. a circle). With this space we know that $\|x_1\|$ and $\|x_3\|$ are bounded. Due to energy being conserved we have

$$E = T + V = \frac{1}{2} m_1 l_1 x_2^2 + \frac{1}{2} m_2 l_2 x_4^2 + \underbrace{V(x_1, x_3)}_{\geq 0}$$
$$E = E_0 = \text{constant} \geq 0.$$

Hence $\|x_2\|$ and $\|x_4\|$ are also bounded, therefore all solutions exist globally.

Definition 2.2. A linear system is one such that for $x \in \mathbb{R}^n$, $A(t) \in \mathbb{R}^{n\times n}$ and $A \in C^0$

$$\boxed{\dot{x} = A(t)x.}$$

Remark 2.4. Note that A can be written as $A = S + \Omega$ where $S = \frac{1}{2}(A + A^T)$ is symmetric (i.e. $S = S^T$) and $\Omega = \frac{1}{2}(A - A^T)$ is skew symmetric (i.e. $\Omega = -\Omega^T$). Furthermore the eigenvalues of S, λ_i, are all real and their respective eigenvectors, e_i, are orthogonal.

Example 2.6 (Global existence in linear systems).

$$\begin{aligned}\langle x, \dot{x}\rangle = \frac{1}{2}\frac{d}{dt}\|x(t)\|^2 &= \langle x, A(t)x\rangle = \langle x, (S(t) + \Omega(t))x\rangle \\ &= \langle x, S(t)x\rangle + \underbrace{\langle x, \Omega(t)x\rangle}_{=0} \overset{(*)}{=} \sum_{i=1}^n \lambda_i(t)x_i^2 \\ &\leq \lambda_{\max}(t)\sum_{i=1}^n x_i^2 = \lambda_{\max}(t)\|x(t)\|^2.\end{aligned}$$

Where in $(*)$ we used that $x = \sum_{i=1}^n x_i e_i$ with $\|e_i\| = 1$ and $e_i \perp e_j$ for all $i \neq j$. Thus we get

$$\frac{\frac{1}{2}\frac{d}{dt}\|x(t)\|^2}{\|x(t)\|^2} \leq \lambda_{\max}(t) \implies \int_{t_0}^t \log\left(\frac{\|x(s)\|^2}{\|x(t_0)\|^2}\right) ds \leq \lambda_{\max}(s)ds.$$

By exponentiating both sides, we obtain

$$\boxed{\|x(t)\| \leq \|x(t_0)\| \exp\left(\int_{t_0}^t \lambda_{\max}(s)ds\right).}$$

Therefore, by the continuation theorem, global solutions exist as long as $\int_{t_0}^t \lambda_{\max}(s)ds < \infty$.

2.4 Dependence on initial conditions

Given the IVP

$$\begin{cases}\dot{x} = f(x,t) \\ x(t_0) = x_0.\end{cases}$$

With $x \in \mathbb{R}^n$ and $f \in C^r$ for some $r \geq 1$, we have the solution $x(t; t_0, x_0)$.

The dependence of the solution on initial data is of interest to us. This is due to us wanting the solution to be robust with respect to errors and uncertainties in the initial data. To address this, we have Theorem 2.5.

Theorem 2.5. *If $f \in C^r$ for $r \geq 1$ then $x(t; t_0, x_0)$ is C^r in (t_0, x_0). Proof in Arnold's book on ODEs.*

The geometric meaning of this is that for $U \subset P \subset \mathbb{R}^n$ we have that $F_{t_0}^t(U)$ is a smooth deformation of U (cf. Fig. 2.7). It turns out $\left(F_{t_0}^t\right)^{-1} = F_t^{t_0}$ is also C^r, hence we have that $F_{t_0}^t$

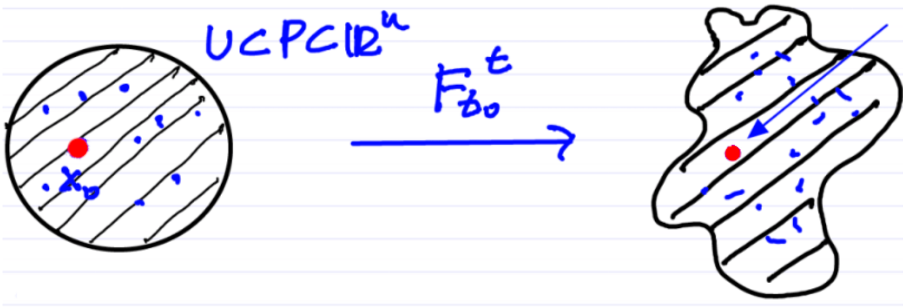

Figure 2.7: The smooth transformation of U. The red point on the right it $F_{t_0}^t(x_0)$, i.e. the image of x_0 under the evolution operator.

is a diffeomorphism.

Remark 2.6 (The total differential). We denote the total differential of a function $f : \mathbb{R}^n \to \mathbb{R}^m$ as Df. The total differential is a function which takes a location x as the argument and returns the derivative of f at the point x, i.e. the Jacobian. This implies evaluating the Jacobian at the point x. For a function $f(x, y) = f(x_1, \ldots, x_n, y_1, \ldots, y_m) : \mathbb{R}^{n+m} \to \mathbb{R}^k$ the total differential Df means with respect to all of the variables and the total differential with respect to x, written $D_x f$ is the total differential only taken with respect to the x variables. Thus for $f(x, y) : \mathbb{R}^{n+m} \to \mathbb{R}$ we have the total differential

$$Df = \begin{pmatrix} \frac{\partial f_1}{\partial x_1} & \cdots & \frac{\partial f_1}{\partial x_n} & \frac{\partial f_1}{\partial y_1} & \cdots & \frac{\partial f_1}{\partial y_m} \\ \vdots & & \vdots & \vdots & & \vdots \\ \frac{\partial f_k}{\partial x_1} & \cdots & \frac{\partial f_k}{\partial x_n} & \frac{\partial f_k}{\partial y_1} & \cdots & \frac{\partial f_k}{\partial y_m} \end{pmatrix};$$

$$Df(x_0, y_0) = \begin{pmatrix} \frac{\partial f_1}{\partial x_1}(x_0, y_0) & \cdots & \frac{\partial f_1}{\partial x_n}(x_0, y_0) & \frac{\partial f_1}{\partial y_1}(x_0, y_0) & \cdots & \frac{\partial f_1}{\partial y_m}(x_0, y_0) \\ \vdots & & \vdots & \vdots & & \vdots \\ \frac{\partial f_k}{\partial x_1}(x_0, y_0) & \cdots & \frac{\partial f_k}{\partial x_n}(x_0, y_0) & \frac{\partial f_k}{\partial y_1}(x_0, y_0) & \cdots & \frac{\partial f_k}{\partial y_m}(x_0, y_0) \end{pmatrix},$$

and the total differential with respect to x

$$D_x f = \begin{pmatrix} \frac{\partial f_1}{\partial x_1} & \cdots & \frac{\partial f_1}{\partial x_n} \\ \vdots & & \vdots \\ \frac{\partial f_k}{\partial x_1} & \cdots & \frac{\partial f_k}{\partial x_n} \end{pmatrix}; \quad D_x f(x_0, y_0) = \begin{pmatrix} \frac{\partial f_1}{\partial x_1}(x_0, y_0) & \cdots & \frac{\partial f_1}{\partial x_n}(x_0, y_0) \\ \vdots & & \vdots \\ \frac{\partial f_k}{\partial x_1}(x_0, y_0) & \cdots & \frac{\partial f_k}{\partial x_n}(x_0, y_0) \end{pmatrix}.$$

Now, how can we compute the Jacobian of the flow map $\frac{\partial x(t;t_0,x_0)}{\partial x_0} = DF_{t_0}^t(x_0)$? We start from the IVP and take the gradient (with respect to x_0) of both sides. On the left hand side we can exchange order of the time derivative and the gradient and on the right hand side we use the chain rule. We end up with the equation

$$\frac{d}{dt}\frac{\partial x}{\partial x_0} = D_x f(x(t;t_0,x_0),t)\frac{\partial x}{\partial x_0}; \quad \frac{\partial x}{\partial x_0} \in \mathbb{R}^{n\times n}.$$

This means, that the flow map gradient satisfies the IVP

$$\begin{aligned} \frac{d}{dt}\left[DF_{t_0}^t(x_0)\right] &= D_x f(F_{t_0}^t(x_0),t) DF_{t_0}^t(x_0) \\ DF_{t_0}^{t_0}(x_0) &= I. \end{aligned}$$

This is called the equation of variations, which is a linear, non-autonomous ODE for the matrix $M = DF_{t_0}^t(x_0)$

$$\begin{cases} \dot{M} = D_x f(x(t;t_0,x_0))M \\ M(t_0) = I. \end{cases}$$

Example 2.7 (Locations of extreme deformation in phase space). We define

$$\begin{aligned} \xi(t) &:= \tilde{x}(t) - x(t) = x(t;t_0,\tilde{x}_0) - x(t;t_0,x_0) \\ &= x(t;t_0,x_0) + \frac{\partial x}{\partial x_0}(t;t_0,x_0)\xi_0 + \mathcal{O}(\|\xi_0\|^2) - x(t;t_0,x_0) \\ &= DF_{t_0}^t(x_0)\xi_0 + \mathcal{O}(\|\xi_0\|^2). \end{aligned}$$

Where we used the Taylor expansion and assume the perturbation to x_0 is small, i.e. $\|\xi_0\| \ll 1$. Therefore we have

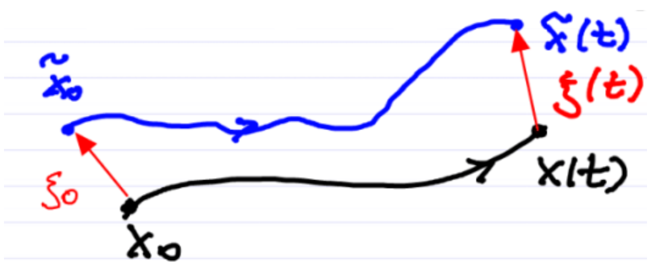

$$\begin{aligned} \|\xi(t)\|^2 &= \langle DF_{t_0}^t(x_0)\xi_0, DF_{t_0}^t(x_0)\xi_0\rangle + \mathcal{O}(\|\xi_0\|^3) \\ &= \langle \xi_0, \underbrace{\left[DF_{t_0}^t(x_0)\right]^T DF_{t_0}^t(x_0)}_{=:C_{t_0}^t(x_0)}\xi_0\rangle + \mathcal{O}(\|\xi_0\|^3). \end{aligned}$$

$C_{t_0}^t(x_0)$ is known as the Cauchy-Green strain tensor. It is positive definite and symmetric and due to its dependence on the initial condition, $C_{t_0}^t(x_0)$ actually defines a *tensor field*. Therefore the largest possible deformation is

$$\max_{x_0,\xi_0} \frac{\|\xi(t)\|^2}{\|\xi_0\|^2} = \max_{x_0,\xi_0} \frac{\langle \xi_0, C_{t_0}^t(x_0)\xi_0 \rangle}{\|\xi_0\|^2} = \max_{x_0} \lambda_n(x_0).$$

Where we used that $C_{t_0}^t$ is positive definite in the last equality, and that $\lambda_n(x_0)$ is the largest eigenvalue of $C_{t_0}^t(x_0)$. Because we typically have exponential growth we introduce the following quantity.

Definition 2.3. The finite-time Lyapunov exponent is defined as

$$\boxed{\mathrm{FTLE}_{t_0}^t(x_0) := \frac{1}{2|t-t_0|} \log(\lambda_n(x_0)).}$$

The FTLE is a diagnostic quantity for Lagrangian Coherent Structures (LCS), i.e. influential surfaces governing the evolution in P.

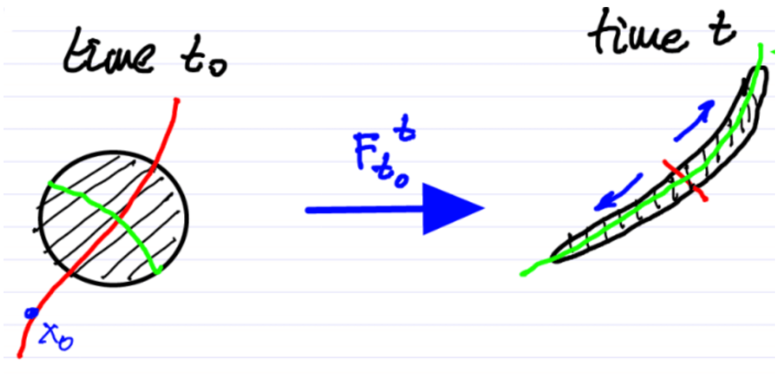

Figure 2.8: On the left the red ridge represents large values of $\mathrm{FTLE}_{t_0}^t$, on the right the green ridge the high values of $\mathrm{FTLE}_t^{t_0}$.

The ridges of $\mathrm{FTLE}_{t_0}^t$ are the repelling LCS, meanwhile the ridges of $\mathrm{FTLE}_t^{t_0}$ are the attracting LCS as depicted in Fig. 2.8. Now we are left with the problem of computing $F_{t_0}^t(x_0)$. Recall that analytically we start with $F_{t_0}^t(x_0)$ and use this to calculate $DF_{t_0}^t(x_0)$. From here we can find $C_{t_0}^t(x_0)$, giving us $\lambda_n(x_0)$ and thereby the FTLE. We now outline a process to compute the FTLE numerically.

(i) Define an initial $M \times N$ grid of initial data $x_0(i,j) \in \mathbb{R}^2$.

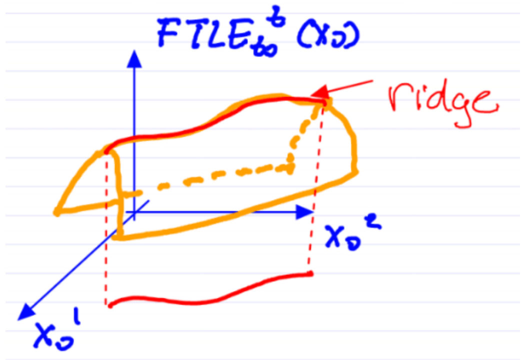

Figure 2.9: The projection of the FTLE ridge onto the initial value space.

(ii) Launch trajectories numerically from grid points to obtain a discrete approximation of $F_{t_0}^t(x_0)$ as $F_{t_0}^t(x_0(i,j))$.

(iii) Use finite differencing to approximate

$$DF_{t_0}^t(x_0(i,j)) \approx \begin{pmatrix} \frac{x(t;t_0,x_0(i,j)+\delta e_1)_1 - x(t;t_0,x_0(i,j)-\delta e_1)_1}{2\delta} & \cdots & \frac{x(t;t_0,x_0(i,j)+\delta e_n)_1 - x(t;t_0,x_0(i,j)-\delta e_n)_1}{2\delta} \\ \vdots & & \vdots \\ \frac{x(t;t_0,x_0(i,j)+\delta e_1)_n - x(t;t_0,x_0(i,j)-\delta e_1)_n}{2\delta} & \cdots & \frac{x(t;t_0,x_0(i,j)+\delta e_n)_n - x(t;t_0,x_0(i,j)-\delta e_n)_n}{2\delta} \end{pmatrix}.$$

This process then yields the surface we see in Fig. 2.9.

Example 2.8 (Calculating the FTLE for the double gyre). Due to incompressibility, we can define the two dimensional flow using a single scalar function called the stream function.

$$\Psi(x,y) = -\sin(\pi x)\sin(\pi y).$$

The components (u, v) of the fluid velocity $(v = (u, v))$ are obtained as partial derivatives of the stream function, according to the formulas

$$\begin{cases} u = \dfrac{\partial \Psi}{\partial y} \\ v = -\dfrac{\partial \Psi}{\partial x}. \end{cases}$$

The Lagrangian trajectories of fluid particles obey the differential equations (i.e. we have the fluid velocity field)

$$\begin{cases} \dot{x} = u = \dfrac{\partial \Psi}{\partial y} \\ \dot{y} = v = -\dfrac{\partial \Psi}{\partial x}. \end{cases}$$

Interestingly, in this case, the phase space coincides with the physical space spanned by the coordinates (x, y).

Remark 2.7. This is an example of a Hamiltonian system, where Ψ is the Hamiltonian (usually denoted as H).

For any autonomous Hamiltonian system we have that the Hamiltonian is constant along trajectories. We can verify this as follows

$$\frac{d}{dt}\Psi(x(t), y(t)) = \frac{\partial \Psi}{\partial x}\dot{x} + \frac{\partial \Psi}{\partial y}\dot{y} = 0.$$

So we have that trajectories are level curves of $\Psi(x, y)$. We can then derive the phase portrait from the level curves of Ψ. Further, we have that $\dot{x} = \frac{\partial \Psi}{\partial y} = -\pi \sin(\pi x)\cos(\pi y)$ which yields that $\text{sign}(\dot{x}) = -\text{sign}(\sin(\pi x))\text{sign}(\cos(\pi y))$. Putting these together we can construct the contour plot with arrows. The contour plot, and FTLE approximation are shown in Fig. 2.10.

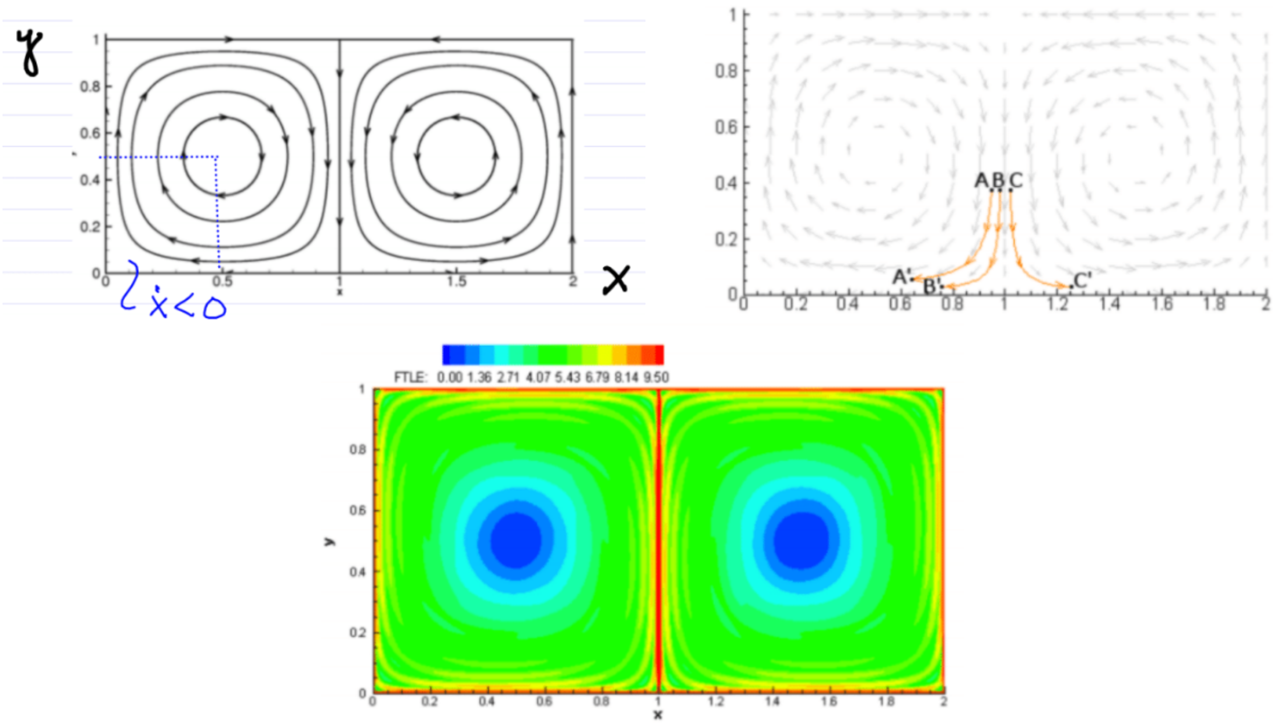

Figure 2.10: Top left: The analytic phase plot. Top right: The exploration done to calculate FTLE. Bottom: The FTLE plot. Figures here were taken from Shawn Shadden of UC Berkeley.

Example 2.9 (ABC flow). Let our dynamical system be defined as follows with $A, B, C \in \mathbb{R}$

$$\begin{cases} \dot{x} = A\sin(z) + C\cos(y) \\ \dot{y} = B\sin(x) + A\cos(z) \\ \dot{z} = C\sin(y) + B\cos(x). \end{cases}$$

This is an exact solution to Euler's equations. We have an autonomous velocity field. Depending on parameters it can even generate chaotic fluid trajectories. The numerical approximation of the FTLE for the ABC flow is depicted in Fig. 2.11.

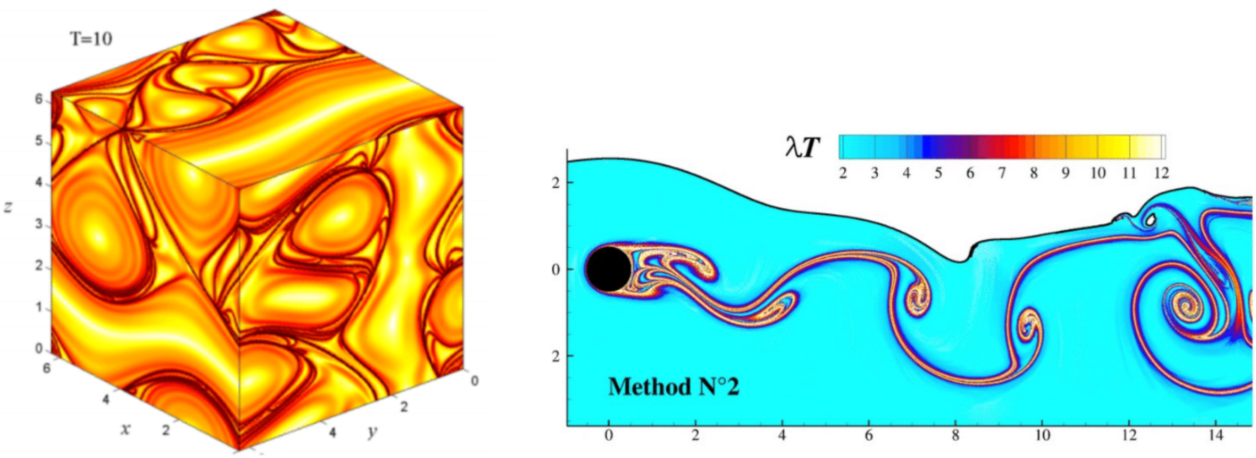

Figure 2.11: Left: numerically calculated FTLE field of the ABC flow. Darker colors signify higher FTLE values (Guckenheimer-Holmes Physica D, 2001). Right: Again the FTLE is plotted, for vortex shedding behind a cylinder under a free surface (Sun et. al, 2016).

2.5 Dependence on parameters

We now have the IVP

$$\begin{cases} \dot{x} = f(x, t, \mu) \\ x(t_0) = x_0. \end{cases}$$

With $x \in \mathbb{R}^n,\ f \in C^r,\ r \geq 1$, therefore we have a solution $x(t; t_0, x_0, \mu) \in C^r_{x_0}$.

We now examine how solutions depend μ. This is critical as solutions should be robust to changes or uncertainties in the model.

Example 2.10 (Perturbation Theory)*.* Given a weakly nonlinear oscillator

$$m\ddot{x} + c\dot{x} + kx = \epsilon f(x, \dot{x}, t),\ 0 \leq \epsilon \ll 1,\ x \in \mathbb{R}.$$

The usual approach is to seek solutions by expanding from the known solution of the linear limit $\epsilon = 0$, i.e.

$$x_\epsilon(t) = \varphi_0(t) + \epsilon\varphi_1(t) + \epsilon^2\varphi_2(t) + \ldots + \mathcal{O}(\epsilon^r).$$

If $x_\epsilon(t)$ is in C^r_ϵ, we have $\varphi_1(t) = \frac{\partial x_\epsilon(t)}{\partial \epsilon}\Big|_{\epsilon=0}$ and $\varphi_2(t) = \frac{\partial^2 x_\epsilon(t)}{\partial \epsilon^2}\Big|_{\epsilon=0}$

Regularity with respect to the parameter μ actually follows from regularity with respect to the initial condition x_0. We can use the following trick to extend the IVP with a dummy variable μ

$$\begin{cases} \dot{x} = f(x, t, u) \\ \dot{\mu} = 0 \\ x(t_0) = x_0 \\ \mu(t_0) = \mu_0. \end{cases}$$

Thus with $X = \begin{pmatrix} x \\ \mu \end{pmatrix} \in \mathbb{R}^{n+p}$ and $F(X_0) = \begin{pmatrix} f \\ 0 \end{pmatrix};\ X_0 = \begin{pmatrix} x_0 \\ \mu_0 \end{pmatrix}$. We have the extended IVP

$$\begin{cases} \dot{X} = F(X) \\ X(t_0) = X_0. \end{cases} \tag{2.1}$$

Applying the previous result on regularity with respect to x_0 to (2.1), we have that $f \in C^r_{x,\mu}$ implies that $X(t) \in C^r_{X_0}$ in turn implying that $x(t; t_0, x_0, \cdot) \in C^r_\mu$. The solution is as smooth in parameters as the RHS of the dynamical system.

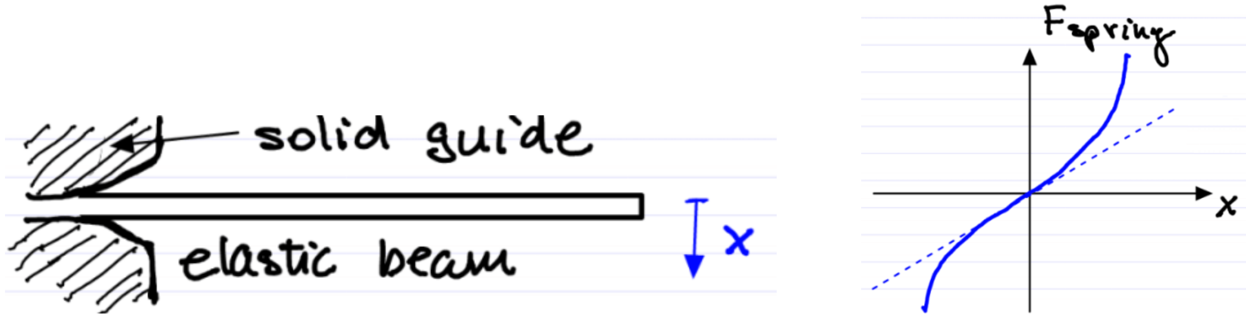

Figure 2.12: Setup for the nonlinear springboard.

Example 2.11 (Periodic Oscillations of a nonlinear springboard). Given an elastic beam extending from a solid guide, we measure the deflection of this beam with the variable x. This system is illustrated in the left panel of Fig. 2.12. By increasing x, the effective free length of the beam is shortened, thereby stiffening the spring nonlinearly. The effect of this nonlinearity on the force exerted on the spring is illustrated in the right panel of Fig. 2.12. This setup yields the following equations of motion

$$\begin{cases} \ddot{x} + x + \epsilon x^3 = 0; \quad 0 \leq \epsilon \ll 1 \\ x(0) = a_0; \quad \dot{x}(0) = 0. \end{cases}$$

So we have weak nonlinearity with no known explicit solution. Although weak, this nonlinearity is still significant, as can be seen in Fig. 2.13. Rewriting this as a first order ODE ($x_1 = x$; $x_2 = \dot{x}$), and note that the RHS is $C^r_{x,\mu}$, therefore there exists a unique local solution that is also C^r_μ. Thus the expansion is justified

$$x_\epsilon(t) = \varphi_0(t) + \epsilon\varphi_1(t) + \ldots + \mathcal{O}(\epsilon^r). \tag{2.2}$$

We can see, by substitution, that for $\epsilon = 0$ we find that $\varphi_0(t) = a_0 \cos(t)$.

Now we look specifically for T-periodic solutions, as we would expect such a solution physically, therefore we have

$$\varphi_i(t) = \varphi_i(t + T).$$

The period T still has to be determined. Plugging this power series into (2.2) into the IVP to get

$$\begin{aligned} \mathcal{O}(1): &\quad \ddot{\varphi}_0 + \varphi_0 &&= 0 \\ \mathcal{O}(\epsilon): &\quad \ddot{\varphi}_1 + \underbrace{\varphi_1}_{\omega=1} &&= -\varphi_0^3 = -a_0^3\cos^3(t) = -a_0^3\left[\frac{1}{4}\cos(3t) + \frac{3}{4}\underbrace{\cos(t)}_{\text{resonance}}\right]. \end{aligned} \tag{2.3}$$

We can see that (2.3) is a linear oscillator with a forcing coming from the zeroth order solution. Since the zeroth order solution $\varphi_0 = a_0 \cos(t)$ already solves the IVP we have the following initial conditions

$$\varphi_1(0) = 0; \quad \dot{\varphi}_1(t) = 0.$$

This holds as $\varphi_0 = a_0 \cos(t)$ already solves the IVP. The general solution to this equation is the sum of two terms. We add the general solution of the homogeneous part and a particular solution to the inhomogeneous part. We can write this solution to (2.3) as

$$\begin{aligned} \varphi_1(t) &= \varphi_1^{\text{hom}}(t) + \varphi_1^{\text{part}}(t) \\ &= \underbrace{A\cos(t) + B\sin(t)}_{\text{TBD from initial conditions}} + \underbrace{C\cos(3t) + Dt\cos(t) + Et\sin(t)}_{\text{TBD from (2.3)}}. \end{aligned}$$

Observe that due to a resonance between the natural frequency of the oscillator and the forcing secular terms, $t\cos(t)$ and $t\sin(t)$ appear. Thus it cannot be periodic, so our Ansatz already fails for $i = 1$. We conclude that no solution of this type exists. Our Ansatz was too restrictive and T should depend on ϵ.

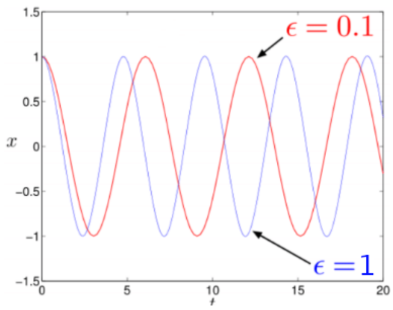

Figure 2.13: Numerical integration of x for $a_0 = 1$ and different values of ϵ.

Lindstedt's idea We should seek a solution of the form

$$x_\epsilon(t) = \varphi_0(t;\epsilon) + \epsilon\varphi_1(t;\epsilon) + \epsilon^2\varphi_2(t;\epsilon) + \mathcal{O}(\epsilon^3).$$

Furthermore φ_i should be T_ϵ periodic, i.e. the period should depend on the strength of the nonlinearity ϵ.

$$\varphi_i(t + T_\epsilon;\epsilon) = \varphi_i(t;\epsilon).$$

Rewriting the period as

$$T_\epsilon = \frac{2\pi}{\omega(\epsilon)}; \quad \omega(\epsilon) = 1 + \epsilon\omega_1 + \epsilon^2\omega_2 + \mathcal{O}(\epsilon^3).$$

We then rescale time according to $\tau = \omega(\epsilon)t$ to find

$$\frac{d}{d\tau} = \frac{1}{\omega(\epsilon)}\frac{d}{dt} \implies \boxed{[\omega(\epsilon)]^2 x'' + x + \epsilon x^3 = 0.}$$

Where we have taken x' to represent $\frac{dx}{d\tau}$. Plugging our expression into the rescaled ODE yields

$$\left(1 + 2\epsilon\omega_1 + \mathcal{O}(\epsilon^2)\right)\left[\varphi_0'' + \epsilon\varphi'' + \mathcal{O}(\epsilon^2)\right] + \left[\varphi_0 + \epsilon\varphi_1 + \mathcal{O}(\epsilon^2)\right] + \epsilon\left[\varphi_0^3 + \mathcal{O}(\epsilon)\right] = 0.$$

Matching equal powers of ϵ yields

$$\begin{aligned}
&\mathcal{O}(1):\ \varphi_0'' + \varphi_0 = 0 \implies \varphi_0(\tau) = a_0\cos(\tau); \quad \varphi_0(0) = a_0; \quad \dot{\varphi}_0(0) = 0\\
&\mathcal{O}(\epsilon):\ \varphi_1'' + \varphi_1 = -\phi_0^3 - 2\omega_1\varphi_0'' = \left(2\omega_1 a_0 - \frac{3}{4}a_0^3\right)\underbrace{\cos(\tau)}_{\text{resonance}} - \frac{a_0^3}{4}\cos(3\tau);\\
&\qquad \varphi_1(0) = 0; \quad \dot{\varphi}_1(0) = 0.
\end{aligned}$$

From the first line, we can see the initial conditions are fulfilled. In this step we used that $\dot{\varphi}(t=0) = 0$ if and only if $\omega(\epsilon)\varphi'(0) = 0$. We get the solution

$$\varphi_1(t) = A\cos(\tau) + B\sin(\tau) + C\cos(3\tau) + D\tau\cos(\tau) + E\tau\sin(\tau).$$

The presence of resonance again excludes periodic solutions, but now we can select ω_1 to eliminate these terms.

$$2\omega_1 a_0 - \frac{3}{4}a_0^3 = 0 \implies \boxed{\omega_1 = \frac{3}{8}a_0^2.}$$

This successfully eliminates the resonance and determines the missing frequency term at $\mathcal{O}(\epsilon)$. Thus we find

$$x_\epsilon(\tau) = a_0\cos(\tau) - \frac{\epsilon}{32}a_0^3\left(\cos(\tau) - \cos(3\tau)\right) + \mathcal{O}(\epsilon^2).$$

In the original time scaling this is

$$x_\epsilon(t) = a_0\cos(\omega t) - \frac{\epsilon}{32}a_0^3\left(\cos(\omega t) - \cos(3\omega t)\right) + \mathcal{O}(\epsilon^2); \quad \omega = 1 + \frac{3}{8}\epsilon a_0^2 + \mathcal{O}(\epsilon^2).$$

This procedure can be continued to higher order terms, where we select ω_2 so that the $\mathcal{O}(\epsilon^2)$ terms cancel.

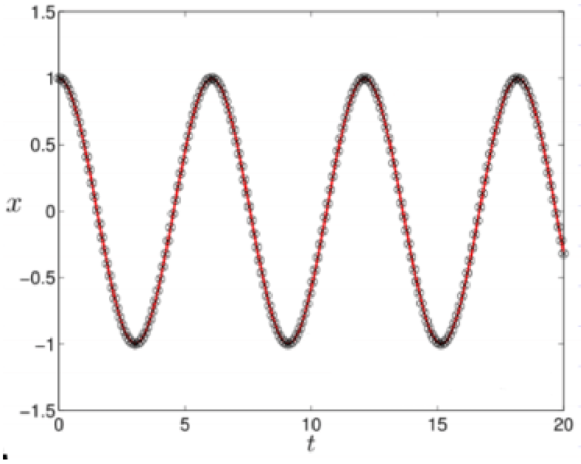

Figure 2.14: Approximation (dots) vs analytic solution (solid line) of x on the time interval $[0, 20]$.

Chapter 3

Stability of fixed points

Now we would like to begin to explore the behaviour of dynamical systems around fixed points. This will allow us to find out if we should expect to observe a fixed state, and to understand what happens if we perturb the system away from this fixed state.

3.1 Basic definitions

Consider

$$\dot{x} = f(x,t), \ x \in \mathbb{R}^n, \ f \in C^1.$$

Assume that $x = 0$ is a fixed point, i.e. $f(0,t) = 0$ for all $t \in \mathbb{R}$. If the fixed point is originally at $x_0 \neq 0$, shift it to zero by letting $\tilde{x} := x - x_0$, therefore

$$\dot{\tilde{x}} = \dot{x} = f(x_0 + \tilde{x}, t) = \tilde{f}(\tilde{x}, t).$$

We would like to understand how the dynamical system behaves near its equilibrium state. To this end we introduce the following definitions.

Definition 3.1 (Lyapupnov Stability)**.** The fixed point $x = 0$ is stable if for all t_0, for all $\epsilon > 0$ small enough, there exists a $\delta = \delta(t_0, \epsilon)$, such that for all $x_0 \in \mathbb{R}^n$ with $\|x_0\| \leq \delta$, we have

$$\boxed{\|x(t; t_0, x_0)\| \leq \epsilon \quad \forall t \geq t_0.}$$

Remark 3.1 (N-dimensional ball). When writing $B(r)$ we refer to the ball of radius r in $\mathbb{R}^n$, i.e. the set $\{x : \ \|x\| < r\}$.

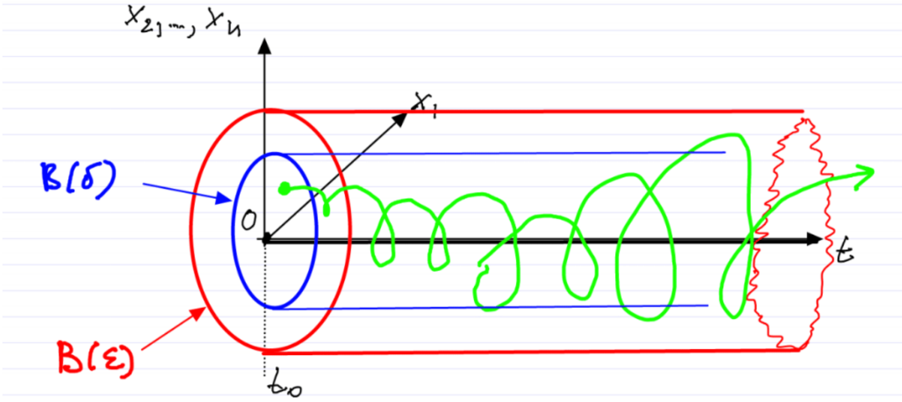

Figure 3.1: An example such a δ for a given Lyapunov stable fixed point.

Example 3.1 (Stability of the lower equilibrium of the pendulum). Recall the equation of motion of the pendulum $\ddot{\varphi} + \sin(\varphi) = 0$, that we transform into a first order ODE by setting $x_1 = \varphi$ and $x_2 = \dot{\varphi}$ to obtain

$$\begin{cases} \dot{x}_1 = x_2 \\ \dot{x}_2 = -\sin(x_1). \end{cases}$$

For small $\epsilon > 0$, this geometric procedure gives a $\delta(\epsilon) > 0$ such that the definition of stability is satisfied for $x = 0$. We can see in Fig. 3.2 that for any initial point chosen within the blue circle, it's trajectory remains within the red circle for all time (cf. Fig. 3.1). Therefore $x = 0$ is (Lyapunov) stable.

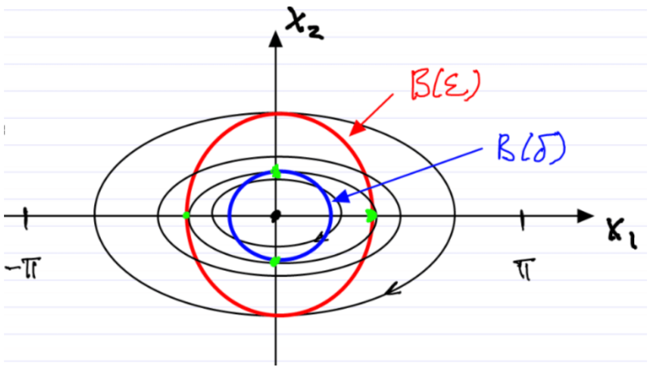

Figure 3.2: Stability of lower equilibrium for the pendulum, here $0 < \epsilon < \pi$.

Definition 3.2 (Asymptotic stability)**.** The fixed point $x = 0$ is *asymptotically stable* if

(i) it is stable,

(ii) for all t_0, there exists $\delta_0(t_0)$ such that for every x_0 with $\|x_0\| \leq \delta_0$ we have

$$\boxed{\lim_{t\to\infty} x(t; t_0, x_0) = 0.}$$

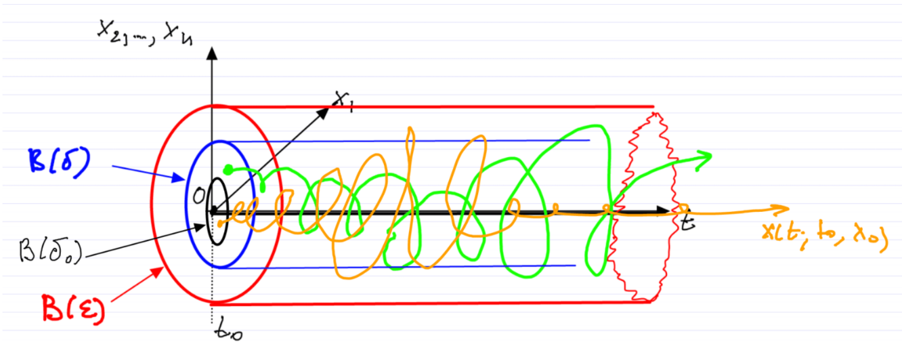

Figure 3.3: An example for an asymptotically stable fixed point (black trajectory).

Definition 3.3 (Domain of attraction)**.** The *domain of attraction* of the fixed point $x = 0$ is the set of all x_0's for which

$$\boxed{\lim_{t\to\infty} x(t; t_0, x_0) = 0.}$$

Example 3.2 (Damped pendulum)*.* We have the equation of motion with the linear damping coefficient c

$$\ddot{\varphi} + c\dot{\varphi} + \sin(\varphi) = 0, \quad c > 0.$$

Transforming into a first-order ODE with $x_1 = \varphi$ and $x_2 = \dot{\varphi}$ gives

$$\begin{cases} \dot{x}_1 = x_2 \\ \dot{x}_2 = -cx_2 - \sin(x_1). \end{cases}$$

The total energy is given by

$$E = \frac{1}{2}x_2^2 + (1 - \cos(x_1)).$$

Further we have the rate of energy change

$$\frac{d}{dt}E(x_1(t), x_2(t)) = x_2(\dot{x}_2 + \sin(x_1)) = -cx_2^2.$$

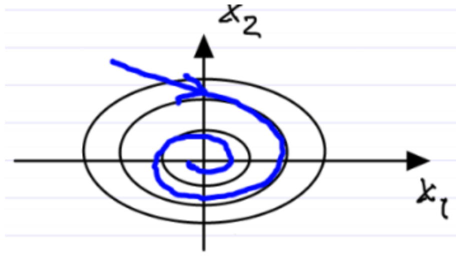

Figure 3.4: An example of a trajectory which loses energy, in this case due to damping.

Therefore, along trajectories energy decreases monotonically as shown in Fig 3.4. By the C^0 dependence of the trajectory on initial conditions, the trajectories remain close to the undamped oscillations for small $c > 0$. We conclude that trajectories are inward spirals for a small dissapation $c > 0$. The fixed point $x = 0$ is still Lyapunov stable, but asymptotic stability does not yet follow (is the limit of $x(t)$ equal to 0?).

Remark 3.2 (LaSalle's invariance principle). This conclusion follows rigorously from LaSalle's invariance principle, namely if we assume that $\dot{x} = f(x)$, $f \in C^1$, and that there exists a $V \in C^1$ with

$$\dot{V} = \frac{dV(x(t))}{dt} \leq 0.$$

Then the set of accumulation points for any trajectory is contained in the set of trajectories that stay within the set $I = \{x \in \mathbb{R}^n : \ \dot{V}(x) = 0\}$.

Example 3.3. Consider the following dynamical system in polar coordinates, i.e. $r\cos(\theta) = x$ and $r\sin(\theta) = y$,

$$\begin{cases} \dot{r} = r(1-r) \\ \dot{\theta} = \sin^2\left(\dfrac{\theta}{2}\right). \end{cases}$$

Note that $r = 0$ is a fixed point, the set $r = 1$ is an invariant circle, and the set $\theta = 0$ is an invariant set. An invariant set is a set such that if the dynamical system is started on the set, it remains in the set for all time. Examining the radial evolution reveals that the equation of motion decouples. We see that $\dot{\theta} \geq 0$, so rotation is either positive or null.

From Fig. 3.5 we can see that both of the fixed points, $(0, 0)$ and $(1, 0)$, are not stable. However, inspecting Fig. 3.5 we see that that $p = (1, 0)$ is an example of an attractor: a set with an open neighborhood of points that all approach the set as $t \to \infty$.

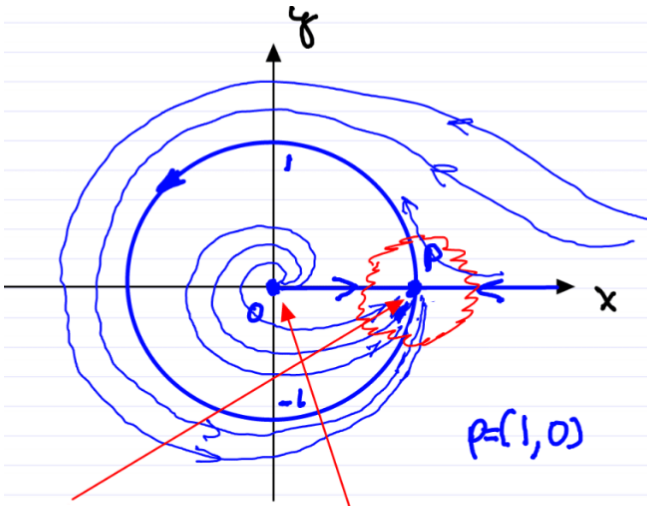

Figure 3.5: Phase portrait of the dynamical system in cartesian coordinates, with the red arrows pointing to the two unstable equilibria.

Definition 3.4 (Invariant set)**.** The set $S \subset P$ is an *invariant set* for the flow map $F^t : P \to P$ if $F^t(S) = S$ for all $t \in \mathbb{R}$.

Definition 3.5 (Unstable point)**.** A fixed point $x = 0$ is unstable if it is not stable.

Remark 3.3. We can negate a mathematical statement by using the reverse relational operators outside the statements involving these operators i.e. $\exists \to \forall$ and $\forall \to \exists$. For example we have for continuity $\forall \epsilon \; \exists \delta : \; \|f(x) - f(y)\| < \epsilon$ if $\|x - y\| < \delta$, meanwhile for discontinuity we have $\exists \epsilon : \; \forall \delta : \; \|f(x) - f(y)\| \geq \epsilon$ for $\|x - y\| < \delta$.

In our case for stability we have

$$\forall \epsilon, t_0 : \quad \exists \delta > 0 : \quad \forall x_0 \text{ with } \|x_0\| < \delta : \quad \|x(t)\| \leq \epsilon \quad \forall t \geq t_0.$$

Meanwhile for instability

$$\exists \epsilon, t_0 : \quad \underbrace{\forall \delta > 0}_{\text{“for arbitrarily small”}} \quad : \quad \exists x_0 \text{ with } \|x_0\| < \delta : \quad \|x(t)\| > \epsilon \quad \underbrace{\exists t \geq t_0}_{\text{“for some”}}.$$

This negation is demonstration in Fig. 3.6.

Remark 3.4. By C^0 dependence of trajectories on initial conditions, if $x(t; t_0, x_0)$ leaves $B(\epsilon)$, then for $\tilde{x}_0$ close enough to x_0, $x(t; t_0, \tilde{x}_0)$ also leaves $B(\epsilon)$. Since this is true on an open set around x_0, the measure of such trajectories in nonzero, the instability is observable!

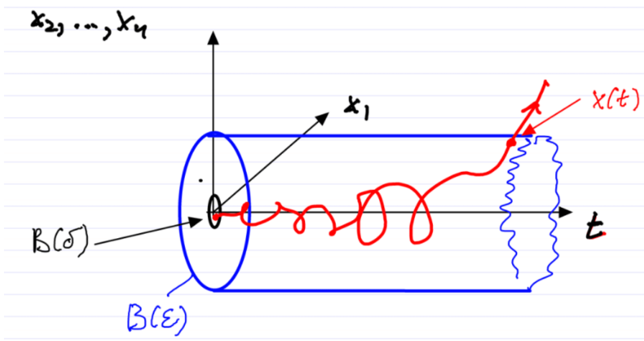

Figure 3.6: Example of an unstable fixed point, with the red trajectory representing a trajectory starting arbitraritly close to the fixed point, leaving a given ϵ-ball.

Example 3.4 (Unstable fixed point of pendulum). In contrast, we can have that infinitely many trajectories converge to the fixed point, yet it is still unstable, as illustrated in Fig. 3.7. In fact, the converging trajectories form a measure-zero set, thus the stability near the unstable equilibrium is unobservable.

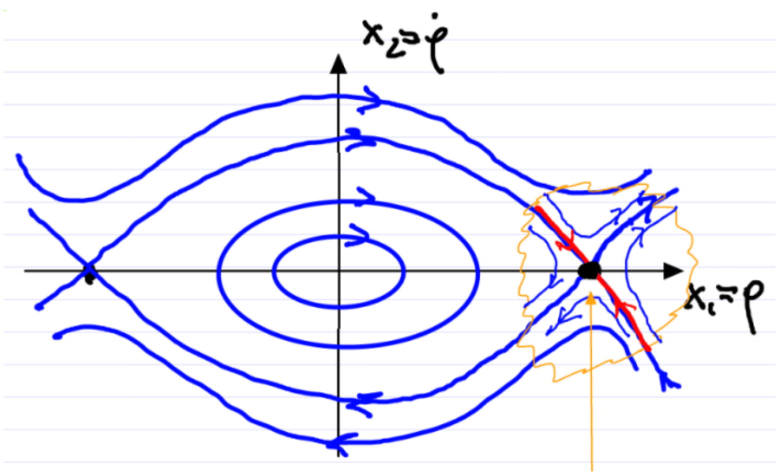

Figure 3.7: The phase portrait around the unstable fixed point of the pendulum, with the stable trajectories (red).

3.2 Stability based on linearization

We would like to derive a more general method to analyze the stability of fixed points, thus we try to simplify our system around the fixed point and discover what this can tell us about the full (unsimplified) system. In the following section we shall always assume that our system is autonomous. We will have the following setup

$$\dot{x} = f(x), \quad f \in C^1, \quad x = \begin{pmatrix} x_1 \\ \vdots \\ x_n \end{pmatrix} \in \mathbb{R}^n, \quad p = \begin{pmatrix} p_1 \\ \vdots \\ p_n \end{pmatrix} \in \mathbb{R}^n. \tag{3.1}$$

If $f(p) = 0$, then p is a fixed point. By transforming using $y = x - p$, we have that in the transformed system $y = 0$ is a fixed point. Furthermore, we have that around $y = 0$ the ODE is

$$\dot{y} = f(p + y) = \underbrace{f(p)}_{=0} + Df(p)y + \mathcal{O}(\|y\|^2) = Df(p)y + \mathcal{O}(\|y\|^2).$$

Definition 3.6 (Linearized ODE)**.** We define the *linearization* of (3.1) at the fixed point p as

$$\boxed{\dot{y} = Ay; \quad y \in \mathbb{R}^n, \quad A := Df(p) \in \mathbb{R}_{n\times n}; \quad Df(p) = \left.\begin{pmatrix} \frac{\partial f_1}{\partial x_1} & \cdots & \frac{\partial f_1}{\partial x_n} \\ \vdots & & \vdots \\ \frac{\partial f_n}{\partial x_1} & \cdots & \frac{\partial f_n}{\partial x_n} \end{pmatrix}\right|_{x=p}.} \tag{3.2}$$

Now we would like to study the stability of the fixed point $y = 0$ in (3.2). From this analysis, we want to know the relevance of our results for the full nonlinear system (3.1).

3.3 Review of linear dynamical systems

Recall the setup

$$\dot{y} = A(t)y, \quad y \in \mathbb{R}^n, \quad A \in \mathbb{R}^{n\times n}, \quad A \in C^0_t.$$

The following facts have already been established

- We know that the global existence and uniqueness of solutions is guaranteed.
- The superposition principle holds; namely the linear combination of solutions is also a solution.

- There exists a set of n linearly independent solutions: $\varphi_1(t), \ldots, \varphi_n(t) \in \mathbb{R}_n$.
- The general solution is

$$y(t) = \sum_{i=1}^{n} c_i \varphi(t) = \underbrace{\begin{bmatrix} \varphi_1(t) & \ldots & \varphi_n(t) \end{bmatrix}}_{\Psi(t)\text{: fundamental matrix solution}} \underbrace{\begin{bmatrix} c_1 \\ \vdots \\ c_n \end{bmatrix}}_{c} = \Psi(t)c; \quad \dot{\Psi} = A(t)\Psi.$$

- We have the initial value problem $y(t_0) = y_0$ which implies

$$\Psi(t_0)c = y_0 \implies y(t) = \underbrace{\Psi(t)\left[\Psi(t_0)\right]^{-1}}_{\phi(t) := F_{t_0}^t} y_0$$

  Where we used that the $\varphi_i(t)$ are linearly independent in the last equality. And we have the *normalized fundamental matrix* $\phi(t)$ equal to the flow map, with $\phi(t_0) = I$.

- In the autonomous case $\dot{x} = Ax$ solutions can be practically constructed.

  (i) **Explicit Solution**

$$\phi(t) = e^{At} := \sum_{j=0}^{\infty} \frac{1}{j!}(At)^j$$

  With $0! = 1$ and $0^0 = I$. We can verify that this is indeed a solution

$$\dot{\phi}(t) = \sum_{j=1}^{\infty} \frac{1}{(j-1)!}(At)^{j-1}A = A\sum_{j=0}^{\infty} \frac{1}{j!}(At)^j = Ae^{At} = A\phi(t).$$

  Where we used that A commutes with its powers in the second equality. We now have that each column of $\phi(t)$ satisfies $\dot{y} = Ay$.

  Remark 3.5. For a scalar ODE $\dot{y} = a(t)y$ for $y \in \mathbb{R}$, the solution is known $y(t) = e^{\int_{t_0}^t a(s)ds} y_0$. However, this does not extend to the higher dimensional $\dot{y} = A(t)y$. In fact, in general, $\phi(t) = e^{\int_{t_0}^t A(s)ds}$ is <u>not</u> a solution. We can check this

$$\dot{\phi} = \sum_{j=0}^{\infty} \frac{1}{j!}\frac{d}{dt}\left(\int_{t_0}^t A(s)ds\right)^j = \sum_{j=1}^{\infty} \frac{1}{(j-1)!}\left(\int_{t_0}^t A(s)ds\right)^{j-1} A(t) \neq A(t)\phi(t).$$

  The nonequality holds as $A(t)$ does not generally commute with $\int A(s)ds$.

(ii) **Solution from eigenfunctions** If we have an autonomous system, we can solve the ODE without an infinite series. We have

$$\dot{y} = Ay, \quad y \in \mathbb{R}^n, \quad y(0) = y_0. \tag{3.3}$$

Substituting $\varphi(t) = e^{\lambda t}s$ for $\lambda \in \mathbb{C}$ and $s \in \mathbb{C}^n$ into (3.3) yields

$$\lambda s = As \implies (A - \lambda I)s = 0 \Longleftrightarrow \det(A - \lambda I) = 0.$$

Therefore λ must be an eigenvalue of A and s must be the corresponding eigenvector. We call $\det(A-\lambda I)$ the *characteristic equation* of A. Let $\lambda_1, \dots, \lambda_n$ be the eigenvalues and $s_1, \dots, s_n$ be the corresponding eigenvectors. In the case that some eigenvalues are repeated, some of the s_i may be generalized eigenvectors. We then have two cases.

(a) A is semisimple, i.e. the eigenvectors are linearly independent (which is always the case if the λ_i all have algebraic multiplicity of one). Then we have the solution

$$y(t) = \sum_{i=1}^{n} c_i e^{\lambda_i t} s_i = \sum_{j=1}^{n} c_j e^{(\mathrm{Re}\lambda_j)t} e^{i(\mathrm{Im}\lambda_j)t} s_j.$$

Where we used $\lambda_j = \mathrm{Re}\lambda_j + i\mathrm{Im}\lambda_j$.

(b) A is <u>not</u> semisimple, i.e. has repeated eigenvalues (but not enough linearly independent eigenvectors). Then we assume that λ_k has algebraic multiplicity $a_k > g_k$, where a_k measures the multiplicity of λ_k as a root of $\det(A - \lambda I) = 0$, and g_k is the number of linearly independent eigenvectors for λ_k, also called the *geometric muliplicity* of λ_k. Even in this case, λ_k gives rise to a_k linearly independent solutions of the form

$$\underbrace{P_0}_{=s_k} e^{\lambda_k t},\ P_1(t)e^{\lambda_k t},\ P_2(t)e^{\lambda_k t}, \dots, P_{a_{k-1}}(t)e^{\lambda_k t}$$

where $P_j(t)$ is a vector polynomial of t of order j or less.

3.4 Stability of fixed points in autonomous linear systems

First we note that we can bound our solution

$$\|y(t)\| = \|\phi(t)y_0\| \leq \underbrace{\|\phi(t)\|}_{\text{Operator norm}} \|y_0\| \leq Ce^{\mu t}\|y_0\|. \tag{3.5}$$

Where $\mu = \max_j(\text{Re}\lambda_j) + \nu$, with $\nu > 0$, as small as needed, provided we increase C appropriately. If A is semisimple, then $\nu = 0$ can be selected.

Theorem 3.6 (Stability of fixed points in linear systems)**.** *Given $y = 0$ a fixed point of the linear system $\dot{y} = Ay$ with $A \in \mathbb{R}^{n\times n}$ the following statements hold:*

(i) Assume that Re$\lambda_j < 0$ for all j. Then $y = 0$ is asymptotically stable.

(ii) Assume that Re$\lambda_j \leq 0$ for all j, and for all λ_k with Re$\lambda_k = 0$ we have $a_k = g_k$. Then $y = 0$ is stable.

(iii) Assume there exists a k such that Re$\lambda_k > 0$. Then $y = 0$ is unstable.

These scenarios are illustrated in Fig. 3.8.

Proof. (i) Pick $\epsilon > 0$, and select $\nu > 0$ small, such that $\mu < 0$. Then pick $C > 0$ such that (3.5) holds, and let $\delta = \frac{\epsilon}{C}$. This implies (since $\|y_0\| \leq \delta$) that

$$\|y(t)\| \leq \epsilon e^{\mu t} \leq \epsilon,$$

and

$$\|y(t)\| \leq \epsilon e^{\mu t} \xrightarrow{t\to\infty} 0.$$

Where the limit holds as $\mu < 0$.

(ii) Again choose $\delta = \frac{\epsilon}{C}$ and note that $\mu = \max_j(\text{Re}\lambda_j) + \nu = 0 + \nu = 0$ ($\nu = 0$ as $a_k = g_k$). Then stability follows by (3.5). However, asymptotic stability does not hold, as $\varphi(t) = Ce^{i(\text{Im}\lambda_j)t}$ solutions exist.

(iii) There exists a solution of the form

$$\varphi(t) = C_k e^{\lambda_k t} s_k = C_k e^{(\text{Re}\lambda_k)t} e^{i(\text{Im}\lambda_k)t} s_k.$$

In turn this implies

$$\|\varphi(t)\| = C_k e^{(\text{Re}\lambda_k)t} \|s_k\| \xrightarrow{t\to\infty} \infty.$$

$\square$

Figure 3.8: Eigenvalue arrangements for scenarios (i), (ii), and (iii) (from left to right) in Theorem 3.6

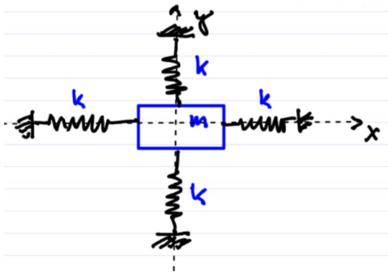

Figure 3.9: Arrangement of coupled oscillators with rectangular mass in the middle.

Example 3.5 (Stability analysis of 2 degrees of freedom coupled oscillators). Given a rectangular mass m with a spring of stiffness coefficient k attached to each side extending to fixed walls in each cardinal direction. We want to know the stability of the equilibrium where all of the springs are equally extended. This dynamical system is depicted in Fig. 3.9. First, note that this is a conservative system, i.e. $E = \text{const}$. Next we transform the coordinates so that the equations of motion can be brought into the form of an ODE for this dynamical system

$$x = \begin{pmatrix} x \\ \dot{x} \\ y \\ \dot{y} \end{pmatrix}.$$

Thus we have a 4-dimensional, nonlinear, system of ODEs. We now linearize this at the fixed point $(x, y) = (0, 0)$, i.e. $\dot{x} = Ax$ with $x \in \mathbb{R}^n$.

The system exhibits full spatial symmetry in x and y, hence the eigenmodes will be the same in the x and y directions. This means we have repeated pairs of purely imaginary eigenvalues for A: $\lambda_{1,2} = \lambda_{3,4} = \pm i\omega$. It is clear that scenarios (i) and (iii) of Theorem 3.6 do not apply to the linearized ODE. So we need to check if (ii) applies.

We have that $\mathrm{Re}\lambda_k = 0$ for $k = 1, 2, 3, 4$. Also $a_k = 2$ for $k = 1, 2, 3, 4$. Now assume $g_k < 2$. Then there would exists solutions of the form $te^{\pm i\omega t}s_k$, but this would contradict the conservation of energy, as either the (nonnegative) kinetic energy and/or the (nonnegative) potential energy would grow unbounded. Hence, the total energy could not be conserved. Therefore we know that $g_k = a_k$ and we can apply (ii) to find $x = y = 0$ is Lyapunov stable for the linearized system. What does this imply for the nonlinear system?

3.5 Stability of fixed points in nonlinear systems

Following the previous example, we would like to know what information about the stability of fixed points of nonlinear systems we can derive from the linearized system. The full nonlinear system is

$$\dot{x} = f(x), \quad f(x_0) = 0, \quad x \in \mathbb{R}^n, \quad f \in C^1. \tag{3.6}$$

And its linearization at the fixed point x_0

$$\dot{y} = Df(x_0)y, \quad y \in \mathbb{R}^n, \quad Df(x_0) \in \mathbb{R}^{n\times n}. \tag{3.7}$$

We would like to conclude that the linearized dynamics are qualitatively similar to the nonlinear dynamics. In order to study if this is the case, we have to formalize *similar* mathematically.

Definition 3.7 (C^k equivalence of dynamical systems)**.** Consider two autonomous dynamical systems:

(i)

$$\dot{x} = f(x), \quad x \in \mathbb{R}^n, \quad f \in C^1; \quad F^t : x_0 \mapsto x(t; x_0). \tag{3.8}$$

(ii)

$$\dot{x} = g(x), \quad x \in \mathbb{R}^n, \quad g \in C^1; \quad G^t : x_0 \mapsto x(t; x_0).$$

The two dynamical systems are C^k *equivalent*, for $k \in \mathbb{N}$, on an open set $U \subset \mathbb{R}^n$, if there exists a C^k diffeomorphism $h : U \to U$ that maps orbits of (i) into orbits of (ii), while preserving the orientation but not necessarily the exact parameterization of the orbit by time. Specifically for all $x \in U$, any $t_1 \in \mathbb{R}$ there exists a $t_2 \in \mathbb{R}$ such that

$$\boxed{h(F^{t_1}(x)) = G^{t_2}(h(x)).}$$

$h : U \to U$ does this for all $x \in U$ in a C^k fashion. This equivalence through a function h is demonstrated in Fig 3.10.

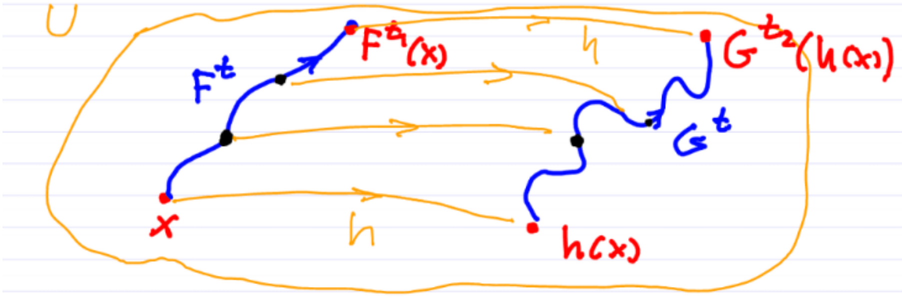

Figure 3.10: The function h mapping the orbits of the dynamical system describing F into the system describing G.

Definition 3.8 (Topological equivalence)**.** For $k = 0$, C^k equivalence is also called *topological equivalence*. In this case, a continuous, invertible deformation takes orbits of one system into the orbits of the other. Under these conditions, $h : U \to U$ is called a *homeomorhpism*.

Example 3.6 (Topologically equivalent linear systems for $n = 2$)*.* To illustrate the meaning of topological equivalence, Fig. 3.11 shows three linear systems ($\dot{x} = Ax$ for $x \in \mathbb{R}^2$) which are topologically equivalent.

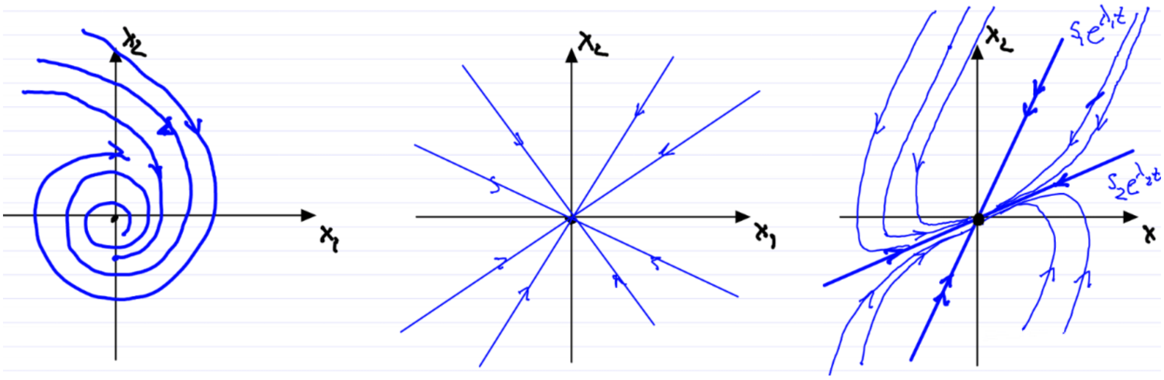

Figure 3.11: Three topologically equivalent 2-dimensional linear systems. Left: The stable spiral. Middle: The sink. Left: The stable node.

The stable spiral has the eigenvalues $\lambda_{1,2} = \alpha \pm i\beta$ for $\alpha < 0$ and $\beta \neq 0$. The sink has the eigenvalues $\lambda_1 = \lambda_2 < 0$. and The stable node has the eigenvalues $\lambda_1 < \lambda_2 < 0$. Note here that the number of eigenvalues λ_i with $\text{Re}\lambda_i < 0$, $\text{Re}\lambda_i = 0$, and $\text{Re}\lambda_i > 0$ is the same is all three of these cases, namely for each system the real part of both eigenvalues are less than 0.

Example 3.7 (Topologically inequivalent linear systems for $n = 2$)*.* As a counter example, we now present three linear systems which are not topologically equivalent. The stable spiral (from before), the unstable spiral, and the saddle. The unstable spiral has the eigenvalues $\lambda_{1,2} = \alpha \pm i\beta$ for $\alpha > 0$ and $\beta \neq 0$ (note the different sign for α). The saddle has the eigenvalues $\lambda_1 < 0 < \lambda_2$. These systems are depicted in Fig 3.12.

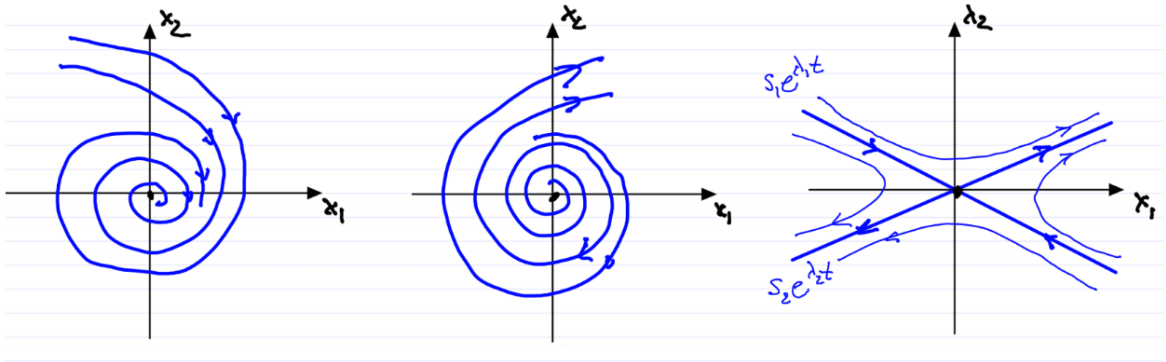

Figure 3.12: Three 2-dimensional linear systems which are not topologically equivalent. Left: The stable spiral. Middle: The unstable spiral. Right: The saddle.

Note here that the eigenvalue configurations in terms of the number of λ_i with real part less than 0 are different in each case. Building on the role of the eigenvalue configuration we noted in the previous examples, we introduce the concept of a hyperbolic fixed point.

Definition 3.9 (Hyperbolic fixed point)**.** We call the fixed point $x = x_0$ a *hyperbolic fixed point* of (3.6) if each of the eigenvalues λ_i of its linearization (3.7) satisfy

$$\boxed{\mathrm{Re}\lambda_i \neq 0.}$$

Geometrically the eigenvalue configuration of a hyperbolic fixed point is shown in Fig. 3.13.

Proposition 3.7. *Under small perturbations to the nonlinear system, the linearized stability type of the hyperbolic fixed point is preserved.*

Before proving this result, recall the Implicit Function Theorem (without proof).

Theorem 3.8 (Implicit Function Theorem ($n+1$ dimensional case))**.** *For a function $F : \mathbb{R}^{n+1} \to \mathbb{R}^1$ which is C^1, if $F(x_0, y_0) = 0$ and the Jacobian $D_x F(x_0, y_0)$ is nonsingular (invertible), then there exists a nearby solution to $F(x, y) = 0$, for $x_y = x_0 + \mathcal{O}(|y - y_0|)$. Further x_y is as smooth in y as $F(x, y)$.*

Proof (Proposition). Add a small perturbation to (3.8) i.e.

$$\dot{x} = f(x) + \epsilon g(x); \quad |\epsilon| \ll 1, \quad f(x_0) = 0.$$

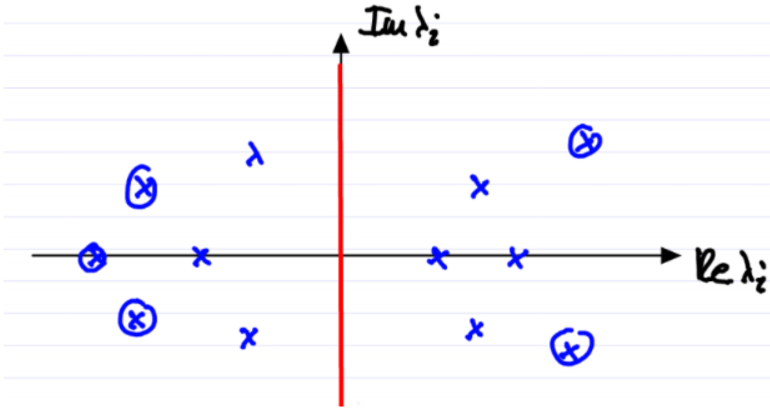

Figure 3.13: The eigenvalue configuration of a hyperbolic fixed point, i.e. no eigenvalues are on the imaginary axis (red).

Now we ask if the perturbed system has a fixed point x_ϵ near x_0. We frame this in terms of the implicit function theorem

$$F(x,\epsilon) = f(x) + \epsilon g(x) \stackrel{?}{=} 0; \quad F(x_0, 0) = 0; \quad x \in \mathbb{R}^n, \quad F: \mathbb{R}^{n+1} \to \mathbb{R}^1.$$

We check that $D_x F(x_0, 0)$ is nonsingular exactly when $Df(x_0)$ is; this is fulfilled as we have no zero eigenvalues. The linearization at the perturbed fixed point takes the form

$$\dot{y} = D\left[f(x) + \epsilon g(x)\right]\big|_{x=x_\epsilon} y = \left[Df(x_0 + \mathcal{O}(\epsilon)) + \epsilon Dg(x_0 + \mathcal{O}(\epsilon))\right] y = \underbrace{\left[Df(x_0) + \mathcal{O}(\epsilon)\right]}_{=A_\epsilon} y.$$

In the last equality we used the Taylor expansion in ϵ. We have that the roots of $\det(A_\epsilon - \lambda I) = 0$ depend continuously on the parameter ϵ. These roots correspond to the eigenvalues of A_ϵ. Therefore, the roots stay within an $\mathcal{O}(\epsilon)$ neighborhood of the eigenvalues of $Df(x_0)$ (see Fig. 3.14). Hence we have that the eigenvalue configuration is unchanged for small enough ϵ. □

Remark 3.9. In the above proof, not only does the hyperbolicity of fixed points remain preserved, but also the stability type.

Meanwhile, for nonhyperbolic fixed points, this is not the case, and the smallest perturbation may change their stability type. This is due to the fact, that no matter how small the scale of the perturbation (ϵ) the $\mathcal{O}(\epsilon)$ ball around eigenvalues on the imaginary axis will always intersect with $\mathbb{C} - \{\mathrm{Im}\lambda_i = 0\}$ (i.e. points which are not on the imaginary axis).

Now we would like to connect the preservation of stability type under nonlinear perturbation to analyzing the stability type of fixed points of nonlinear dynamical systems based on their linearization.

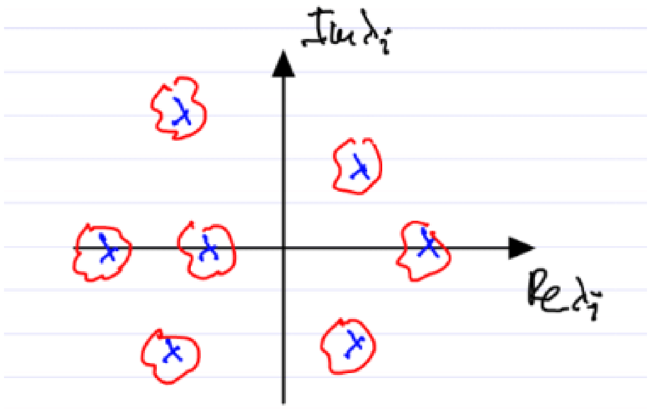

Figure 3.14: The eigenvalue configuration the $\mathcal{O}(\epsilon)$ neighborhood (red) drawn around each eigenvalue (blue).

Theorem 3.10 (Hartman-Grobman)**.** *If the fixed point x_0 of the nonlinear system* (3.6) *is hyperbolic, then the linearization* (3.7) *is topologically equivalent to the nonlinear system in a neighborhood of x_0.*

Consequence: *For hyperbolic fixed points, linearization predicts the correct stability type and orbit geometry near x_0.*

Now we would like to apply this to the pendulum to systematically derive the stability type of its fixed points.

Example 3.8 (Stability analysis of the pendulum via Hartman-Grobman)*.* Recall the transformed ODE for the pendulum

$$\dot{x} = f(x) = \begin{cases} \dot{x}_1 = x_2 \\ \dot{x}_2 = -\sin(x_1) \end{cases}; \quad x = \begin{pmatrix} x_1 \\ x_2 \end{pmatrix}.$$

We have two fixed points $p = (\pi, 0)$ and $q = (0, 0)$. First we analyze the stability of the fixed point p. The differential of f at a point a is

$$Df(a) = \begin{pmatrix} 0 & 1 \\ -\cos(a_1) & 0 \end{pmatrix}.$$

Start by linearizing at p

$$\dot{y} = Ay; \quad A = Df(p) = \begin{pmatrix} 0 & 1 \\ -\cos(x_1) & 0 \end{pmatrix}_{x=p} = \begin{pmatrix} 0 & 1 \\ 1 & 0 \end{pmatrix}.$$

Now we have to check if p is hyperbolic

$$\det(A-\lambda I)=\lambda^2-1=0 \implies \lambda_{1,2}=\pm 1;\ s_1=\begin{pmatrix}1\\1\end{pmatrix},\ s_2=\begin{pmatrix}-1\\1\end{pmatrix}.$$

Neither of the eigenvalues lie on the imaginary axis, so p is hyperbolic. This allows us to move between the nonlinear and linearized system for the stability analysis without compromising our results. We find the linearized dynamics to be

$$y(t)=C_1e^t s_1+C_2e^{-t}s_2.$$

Using the initial conditions y_0 the trajectory can be expressed as

$$y(t)=F^t y_0,$$

where F^t is the normalized fundamental matrix solution. We can now fully describe the phase portrait of the linearization. The *stable subspace* E^S is span$\{s_2\}=\{y_0:\ F^t y_0 \xrightarrow{t\to\infty} 0\}$. The unstable subspace E^U is span$\{s_1\}=\{y_0:\ F^t y_0 \xrightarrow{t\to-\infty} 0\}$. The phase portrait near the fixed point p is illustrated in Fig. 3.15

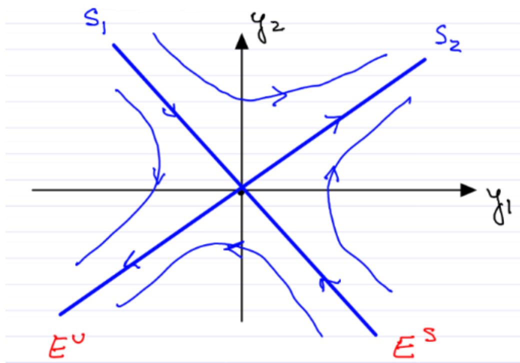

Figure 3.15: The phase portrait of the linearized pendulum in a neighborhood around p.

The nonlinear phase portrait is topologically equivalent to the linear one. Further we can define the stable and unstable manifolds of p for the nonlinear system. We designate $F^t(\cdot)$ to be the flow map for the nonlinear system after this point. The *stable manifold* of p is

$$\boxed{W^S=\{x_0:\ F^t(x_0)\xrightarrow{t\to\infty} p\}.}$$

and the *unstable manifold* of p

$$\boxed{W^U=\{x_0:\ F^t(x_0)\xrightarrow{t\to-\infty} p\}.}$$

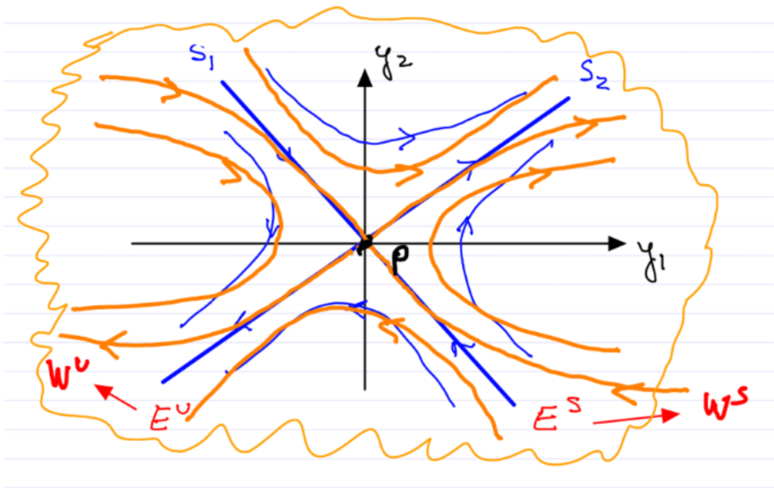

Figure 3.16: The phase portrait of the pendulum on a neighborhood around p with the stable and unstable manifolds of the nonlinear system as well as the stable and unstable spaces of the linearization.

Both of these are C^0 curves through p and their existence follows from the Hartman-Grobman theorem. These manifolds are shown in the nonlinear phase portrait around p in Fig. 3.16.

Next we analyze the stability of the fixed point q. Once again, our first step is to linearize

$$\dot{y} = Ay, \quad A = Df(q) = \begin{pmatrix} 0 & 1 \\ -1 & 0 \end{pmatrix}; \quad \det(A - \lambda I) = 0.$$

From here, we see that the determinant is equal $\lambda^2 + 1 = 0$, yielding the roots $\lambda_{1,2} = \pm i$, i.e. the fixed point is <u>not</u> hyperbolic. Thus the linearized dynamics is inconclusive for the nonlinear system. In this particular case, q turns out to be stable by the definition of Lyapunov stability. Later we will use another approach to show this directly.

In the last example, the importance of hyperbolicity was not accentuated, as the latter fixed point had the same stability type in the linearized system as in the full system. This leads us to question if there are cases where the stability type between the linear and nonlinear systems is not preserved.

Example 3.9 (Criticality of hyperbolicity in Hartman-Grobman). Let the dynamical system be

$$\dot{x} = ax^3, \quad x \in \mathbb{R}, \quad a \neq 0.$$

This system has a fixed point at $x = 0$, linearizing here gives

$$A = 3ax^2\big|_{x=0} = 0 \implies \dot{y} = 0y = 0.$$

We have a single root $\lambda_1 = 0$, hence $x = 0$ is a nonhyperbolic fixed point. Disregarding this fact, we may be inclined to conclude that $x = 0$ is a stable fixed point, since $y = 0$ is trivially a fixed point of the linearization $\dot{y} = 0$. This is not the case, as we can see by analyzing the full nonlinear dynamics for $a > 0$ as in Fig. 3.17, where we observe that $x = 0$ is an unstable fixed point.

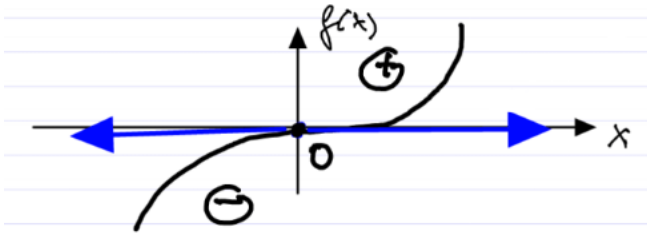

Figure 3.17: Nonlinear dynamics for the dynamical system $\dot{x} = ax^3$ with $a > 0$.

Now that we have understood how to use the Hartman-Grobman theorem, we would like to to be able to definitely conclude the stability type of a fixed point, once we have the linearization. To achieve this, we require a sufficient and necessary criterion for all of the eigenvalues of the linearized system to be left of the imaginary axis, i.e. $\text{Re}\lambda_i < 0$ for all i.

Theorem 3.11 (Routh-Hurwitz). *Consider the polynomial*

$$a_n\lambda^n + a_{n-1}\lambda^{n-1} + \ldots + a_1\lambda + a_0 = 0.$$

Without loss of generality assume $a_0 > 0$, if $a_0 < 0$ then multiply by -1 and if $a_0 = 0$ then $\lambda = 0$ is a root and therefore we cannot have asymptotic stability. Next, define the following series of subdeterminants

$$D_0 = a_0,\ D_1 = a_1,\ D_2 = \begin{vmatrix} a_1 & a_0 \\ a_3 & a_2 \end{vmatrix},\ D_3 = \begin{vmatrix} a_1 & a_0 & 0 \\ a_3 & a_2 & a_1 \\ a_5 & a_4 & a_3 \end{vmatrix}, \ldots,\ D_n = \begin{vmatrix} a_1 & a_0 & 0 & \ldots & 0 \\ a_3 & a_2 & a_1 & \ldots & 0 \\ \vdots & & & & \vdots \\ 0 & \ldots & a_n & a_{n-1} & a_{n-2} \\ 0 & \ldots & & 0 & a_n \end{vmatrix}$$

Then we have that if and only if for all i $D_i > 0$ then $Re\lambda_i < 0$ for all i.

A weaker neccesary condition is that if for all i $Re\lambda_i < 0$ then $a_i > 0$ for all i. Therefore if there exists an $a_k < 0$, we know immediately that the fixed point cannot be asymptotically stable as not all of the $Re\lambda_i$ can be strictly negative.

Remark 3.12. For a given i we construct the matrix used for calculating D_i as follows: write the elements $a_1, \ldots, a_i$ along the diagonal, then in each row k write the a_j in descending index order such that a_k aligns with the placement inherited from us writing along the diagonal. The leftover spaces are filled with zeros.

Remark 3.13. Adolf Hurwitz discovered this criterion independently of Edward Routh in 1895 while holding a chair at the ETH.

Example 3.10 (Applying the Routh-Hurwitz criterion). Given the polynomial

$$a_3\lambda^3 + a_2\lambda^2 + a_1\lambda + a_0 = 0.$$

The Routh-Hurwitz criterion is

$$D_0 = a_0 > 0;\ D_1 = a_1 > 0;\ D_2 = a_1a_2 - a_0a_3 > 0;\ D_3 = a_3D_2 > 0.$$

Therefore

$$\boxed{a_0 > 0,\ a_1 > 0,\ a_1a_2 - a_0a_3 > 0,\ a_3 > 0}$$

forms a sufficient and necessary condition for asymptotic stability ($a_i > 0$ follows from here) for $n = 3$.

Example 3.11 (Watt's centrifugal governor for steam engines). Now we put together everything built until now in the example of Watt's centrifugal governor for steam engines. Originally this system was used in mills in the 1700's, then it was adapted by Watt to the steam engine in 1788. This adaptation has been credited as a major factor in the industrial revolution, and is a first example of feedback control. The system is outlined in Fig. 3.18. The two masses (of mass $\frac{m}{2}$) rotate counter clockwise, and their position in radians is given by θ, with their rotational velocity $\dot{\theta}$. The masses are attached by a rod of length L and their deflection from the vertical position is measured by φ. Smaller $\dot{\theta}$ allowed for an increase in steam supply.

Following changes in the design, the systems suddenly became unstable. To address this Vishnegradky studied the root cause in 1877. We first derive the equation of motion. For the governor we use the equation of motion for a rotating hoop (with viscous damping coefficient b).

$$mL^2\ddot{\varphi} + bL^2\left(\frac{g}{L} - \dot{\theta}^2\cos(\varphi)\right)\sin(\varphi) = 0; \quad b > 0.$$

Next, let ω denote the angular velocity of the steam engine, i.e. with the gear ratio n we have $\dot{\theta} = n\omega$. Then we find

$$m\ddot{\varphi} = -b\dot{\varphi} - m\left(\frac{g}{L} - n^2w^2\cos(\varphi)\right)\sin(\varphi).$$

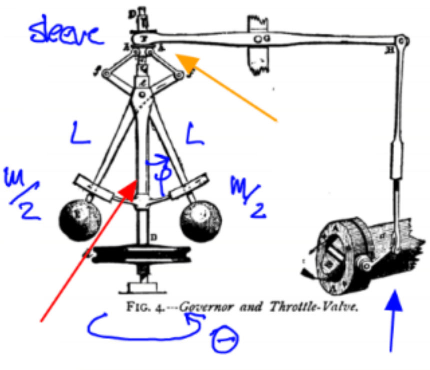

Figure 3.18: Schematic for Watt's centrifugal governor. The yellow arrow points towards a damper on the rotation about the spindle (red arrow). On the right the blue arrow designates a steam engine cylinder.

Now we derive the equation of motion for the steam engine. Denote the moment of inertia for the engine by J, the driving torque from the steam as P_1 and the constant load P, we obtain

$$J\dot{\omega} = P_1 - P.$$

In this case we have $P_1 = P^* + k\left(\cos(\varphi) - \cos(\varphi^*)\right)$ for the desired operation angle φ^*, the gain k, and $P*$ the value of P at φ^*. Putting this together yields

$$J\dot{\omega} = k\cos(\varphi) - P_0; \quad P_0 = P - P^* + k\cos(\varphi^*).$$

Let $\dot{\varphi} = \Psi$ to transform into a three-dimensional set of equations (ODE)

$$\begin{cases} \dot{\varphi} = \Psi \\ \dot{\Psi} = -\dfrac{b}{m}\Psi - \left(\dfrac{g}{L} - n^2\omega^2\cos(\varphi)\right)\sin(\varphi)\,; \\ \dot{\omega} = \dfrac{k}{J}\cos(\varphi) - \dfrac{P_0}{J}. \end{cases} \quad x = \begin{pmatrix} \varphi \\ \Psi \\ \omega \end{pmatrix}.$$

Then our operation point is the fixed point x_0 of this system

$$f(x_0) = 0 \implies \Psi_0 = 0;\ \omega_0^2 = \frac{g}{Ln^2\cos(\varphi_0)};\ \cos(\varphi_0) = \frac{P_0}{k}.$$

If $\sin(\varphi_0) = 0$, we have an unphysical state and ignore this case. For simplification set $L = 1$, this could be formally achieved by nondimensionalizing the length L. Now we linearize at the fixed point x_0

$$\dot{y} = Ay; \quad A = Df(x_0) = \begin{pmatrix} 0 & 1 & 0 \\ n^2\omega^2\cos(2\varphi_0) - g\cos(\varphi_0) & -\frac{b}{m} & n^2\omega_0\sin(2\varphi_0) \\ -\frac{k}{J}\sin(\varphi_0) & 0 & 0 \end{pmatrix}.$$

With this we obtain the characteristic equation $\det(A - \lambda I) = 0$

$$\underbrace{1}_{a_3}\lambda^3 + \underbrace{\frac{b}{m}}_{a_2}\lambda^2 + \underbrace{g\frac{\sin^2(\varphi_0)}{\cos(\varphi_0)}}_{a_1}\lambda + \underbrace{g\frac{2k\sin^2(\varphi_0)}{J\omega_0}}_{a_0} = 0.$$

Now check the Routh-Hurwitz criterion for asymptotic stability:

(i) The necessary condition for $\mathrm{Re}\lambda_k < 0$ for all k: $a_j > 0$ for all j is fulfilled.

(ii) Next we check the subdeterminants

$$\begin{aligned} D_0 &= a_0 = g\frac{2k\sin^2(\varphi_0)}{J\omega_0} > 0; \\ D_1 &= a_1 = g\frac{\sin^2(\varphi_0)}{\cos(\varphi_0)} > 0; \\ D_2 &= \begin{vmatrix} a_1 & a_0 \\ a_3 & a_2 \end{vmatrix} = a_1a_2 - a_0a_3 = g\frac{b}{m}\frac{\sin^2(\varphi_0)}{\cos(\varphi_0)} - g\frac{2k\sin^2(\varphi_0)}{J\omega_0} > 0; \\ D_3 &> 0 \iff D_2 > 0 \text{ and } a_3 = 1 > 0. \end{aligned}$$

The only actual condition for x_0 to be asymptotically stable is $D_2 > 0$

$$\frac{bJ}{m} > \frac{2P_0}{\omega_0}.$$

From the equation for the fixed points we know

$$P_0\omega_0^2 = \frac{gk}{n^2} = \text{const.} \tag{3.9}$$
$$\omega_0^2 + 2P_0\omega_0\frac{d\omega_0}{dP_0} = 0.$$

From the first equation, we realize that we must write $\omega_0 = \omega_0(P_0)$. To obtain the second equation, we derive the first equation (3.9) with respect to P_0. Therefore we find

$$\frac{d\omega_0}{dP_0} = -\frac{\omega_0}{2P_0}.$$

Next, define the *non-uniformity of performance*

$$\nu = \left|\frac{d\omega_0}{dP_0}\right| = \frac{\omega_0}{2P_0}.$$

Then our criterion for asymptotic stability becomes

$$\frac{bJ}{m}\nu > 1.$$

To conclude, the following have harmful effects of stability

- Bigger engines which increase m
- Better machining of surfaces decreasing b
- Increased operating speed decreasing J
- Versatility in operation decreasing ν.

These have the effect of pushing the eigenvalues to the right in the complex plane (towards the imaginary axis) as is illustrated in Fig 3.19.

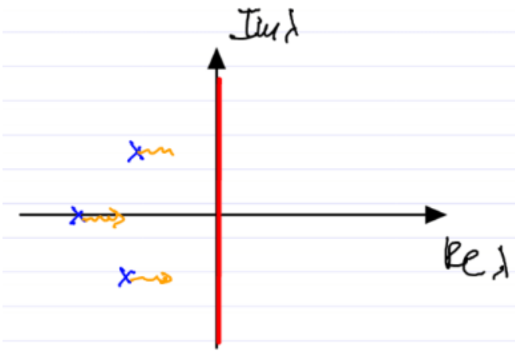

Figure 3.19: Change in the eigenvalue configuration as small modification are made to the Watt engine governor.

3.6 Lyapunov's direct (second) method for stability

Stability analysis via linearization is not perfect. For nonhyperbolic fixed points, the results obtained are inconclusive, and this case turns out to be somewhat common for conservative systems. Furthermore, linearization does not give any insight into the size of the domain of stability. Hence, a method for determining stability type without relying on linearization would be desirable. This is given to us by Lyapunov's direct method.

Theorem 3.14. *Consider*

$$\dot{x} = f(x), \quad f \in C^1, \quad x \in \mathbb{R}^n; \quad f(x_0) = 0.$$

Assume that there exists a function $V : U \to \mathbb{R}$ with $V \in C^1(U)$ for an open set $U \subset \mathbb{R}^n$ and $x_0 \in U$ which fulfills the following

(i) V is positive definite in a neighborhood of x_0, i.e.

$$V(x_0) = 0; \quad V(x) > 0, \ x \in U - \{x_0\}.$$

(ii) $\dot{V}$ is negative semidefinite in the same neighborhood, i.e.

$$\dot{V} = \frac{d}{dt}V(x(t)) = \langle DV(x(t)), \dot{x}(t)\rangle = \langle DV(x(t)), f(x(t))\rangle \leq 0, \ x \in U.$$

Then $x = x_0$ is Lyapunov stable (cf. Def. 3.1). V is called a Lyapunov function. The hypotheses are illustrated in Fig. 3.20.

Remark 3.15. To denote the boundary of a set A we write ∂A.

Proof. First choose $\epsilon > 0$ and define $\alpha(\epsilon) = \min_{x \in \partial B_\epsilon(x_0)} V(x) > 0$. Note that $\alpha(\epsilon)$ is well defined as $V \in C^0(U)$ and $\partial B_\epsilon(x)$ is compact and spherical for small enough ϵ. There exists an $x^* \in \partial B_\epsilon(x)$ with $V(x^*) = \alpha(\epsilon) \leq V(x)$ for all $x \in \partial B_\epsilon(x_0)$. Next, define $U_\epsilon = \{x \in B_\epsilon(x_0) : V(x) < \alpha(\epsilon)$. Notice that $x_0 \in U_\epsilon$ because $V(x_0) = 0$ and $V(x) \geq 0$ on U. Further U_ϵ is open due to the continuity of V. We have that $U_\epsilon \cap \partial B_\epsilon(x_0)$ is empty by definintion, noting that for all $x \in \partial B_\epsilon(x_0)$ we have $V(x) \geq \alpha(\epsilon)$. Therefore there exists a ball $B_{\delta(\epsilon)} \subset U_\epsilon$ which contains x_0. This can be seen in Fig. 3.21.

Now observe that for every $\tilde{x}_0 \in B_{\delta(\epsilon)}(x_0)$ we have that along trajectories $V(x(t;\tilde{x}_0)) \leq V(\tilde{x}_0) < \alpha(\epsilon)$. The first inequality comes from hypothesis (ii) and the second inequality from the definition of U_ϵ. This implies that for $x(t;\tilde{x}_0) \in U_\epsilon$ we have that $x(t;\tilde{x}_0)$ is not in $\partial B_\epsilon(x_0)$ for any $t > 0$. The trajectory $x(t;\tilde{x}_0)$ is continuous, in order for it to leave the ball $B_\epsilon(x_0)$ it must intersect the boundary $\partial B_\epsilon(x_0)$. At this point $V(x)$ will atain a value of at least $\alpha(\epsilon)$ by definition, however this is in contradiction to the fact that $V(x(t;\tilde{x}_0))$ is strictly smaller that $\alpha(\epsilon)$. Therefore must stay in the ball $B_\epsilon(x_0)$ for all times. $\square$

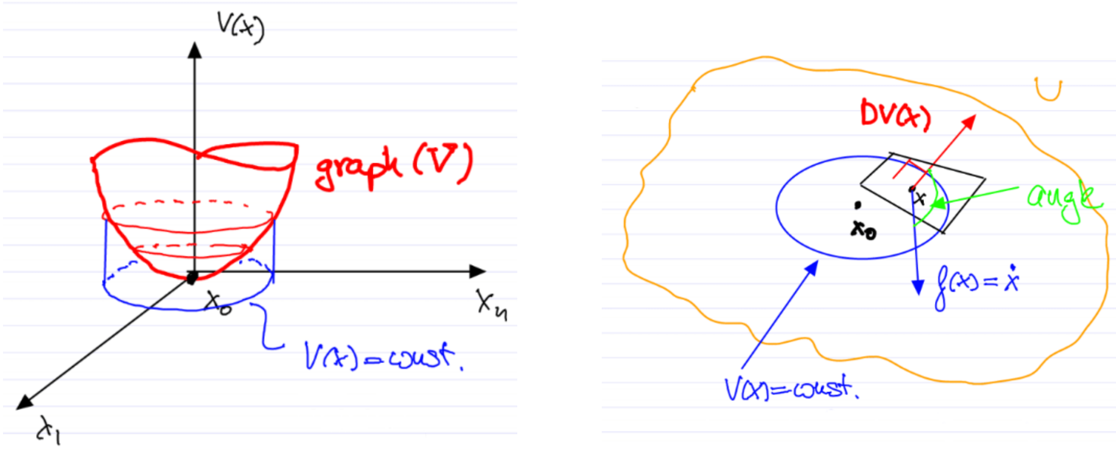

Figure 3.20: Geometric interpretation of hypotheses of Lyapunov's direct method. Left depicts hypothesis (i) and right hypothesis (ii). The angle between $DV(x)$ and $f(x)$ is at least $\frac{\pi}{2}$. In each image the blue $V(x)$ =const. is a level surface diffeomorphic to S^{n-1}.

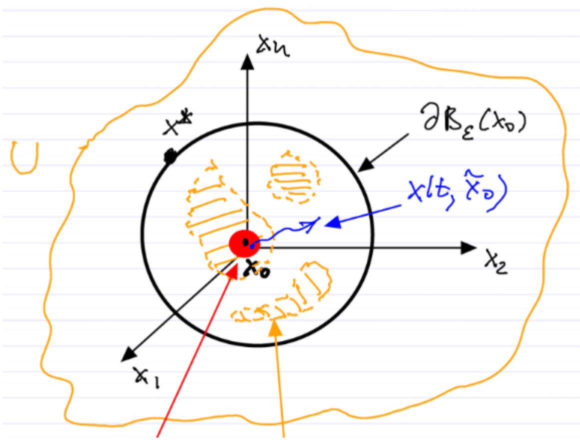

Figure 3.21: The constellation of U, U_ϵ, $\partial B_\epsilon(x_0)$, and $B_{\delta(\epsilon)}(x_0)$ from the proof of Lyapunov's direct method. The red arrow points at $B_{\delta(\epsilon)}(x_0)$ and the yellow arrow at a connected component of U_ϵ.

Now we present some extensions to this theorem for various different stability types. These are necessary, as the previous theorem only provides a sufficient condition for stability (it is not "if and only if").

Theorem 3.16 (Theorem 2)**.** *Consider the same dynamical system. Assume*

(i) $V(x)$ *is positive definite,*

(ii) $\dot{V}(x)$ *is negative definite, i.e.*

$$\dot{V}(x) < 0, \;\; x \in U - \{x_0\}.$$

Then $x = x_0$ *is asymptotically stable. These hypotheses are illustrated in Fig. 3.22.*

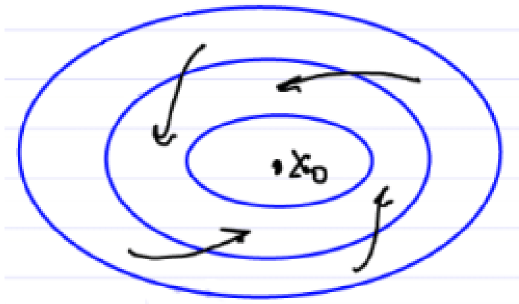

Figure 3.22: The hypotheses of Theorem 2 illustrated, the key difference being that the arrows (denoting the flow of the dynamical system) cross the level surfaces of V (blue rings) toward x_0.

Theorem 3.17 (Theorem 3)**.** *Consider the same dynamical system. Assume*

(i) $V(x)$ *is positive definite,*

(ii) $\dot{V}(x)$ *is positive definite, i.e.*

$$\dot{V}(x) > 0, \;\; x \in U - \{x_0\}.$$

Then $x = x_0$ *is unstable. The hypotheses are illustrated in Fig. 3.23.*

Theorem 3.18 (Theorem 4)**.** *Consider the same dynamical system. Assume*

(i) $V(x)$ *is indefinite, i.e. arbitrarily close to* x_0 *there exists* $a, b \in U$ *such that* $V(x_1) \cdot V(x_2) < 0$ *(they have opposite signs and are not equal to 0) and* $V(x_0) = 0$.

(ii) $\dot{V}(x)$ *is definite near* x_0 *(either positive or negative).*

Then $x = x_0$ *is unstable. The geometry of the hypotheses are illustrated in Fig. 3.24.*

Remark 3.19. In each of these theorems, the definiteness of $\dot{V}$ can be replaced by semidefiniteness, if we add that the set $\{x \in U : \; \dot{V}(x) = 0\}$ does not contain full trajectories of the system. This is called Krasovsky's condition.

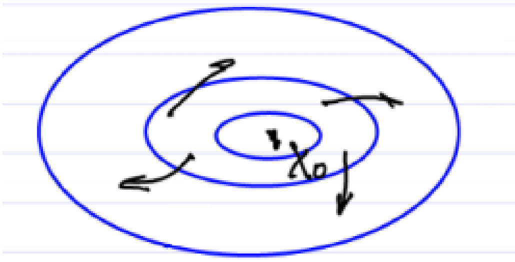

Figure 3.23: The hypotheses of Theorem 3 illustrated, the key difference being that the arrows (denoting the flow of the dynamical system) cross the level surfaces of V (blue rings) away from x_0.

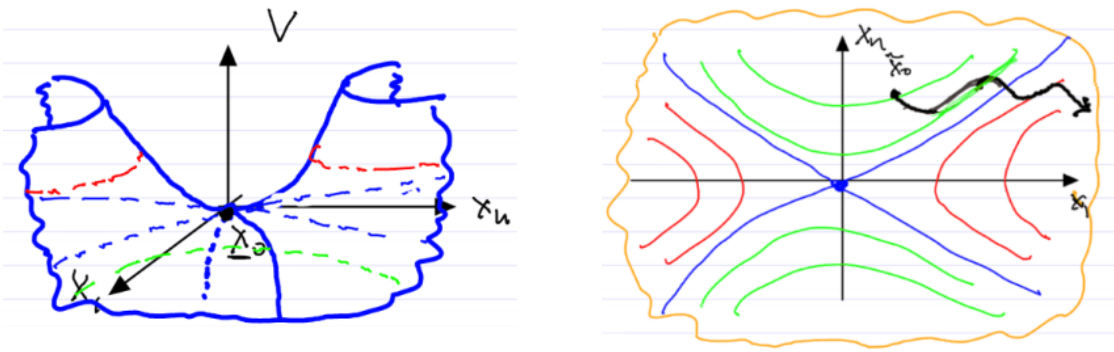

Figure 3.24: The geometry of hypotheses (i) (left) and (ii) (right) for $\dot{V}$ positive definite of Theorem 4 illustrated. On the right level surfaces are designated by lines, blue corresponds to $V = 0$, red $V > 0$, and green $V < 0$, which can be seen as the dotted lines of the same colors on the left.

Now we would like to put these theorems into practice with a few examples.

Example 3.12 (Stability analysis of the pendulum with Lyapunov's direct method)*.* Recall that using linearization, we were only able to conclude the stability type of one of the fixed points for the dynamical system of the pendulum

$$ml^2\ddot{\varphi} + mgl\sin(\varphi) = 0.$$

Now we will use the energy as a Lyapunov function, which is often very useful. The energy is given by

$$E(x) = E(\varphi, \dot{\varphi}) = \frac{1}{2}ml^2\dot{\varphi}^2 + mgl(1 - \cos(\varphi)) = \frac{1}{2}ml^2\dot{x_2}^2 + mgl(1 - \cos(x_1)).$$

Transforming the dynamical system to be an system of first order ODEs we obtain

$$x = \begin{pmatrix} x_1 \\ x_2 \end{pmatrix} = \begin{pmatrix} \varphi \\ \dot{\varphi} \end{pmatrix}; \quad \dot{x} = \begin{pmatrix} \dot{x}_1 \\ \dot{x}_2 \end{pmatrix} = \begin{pmatrix} x_2 \\ -\frac{g}{l}\sin(x_1) \end{pmatrix} = f(x).$$

At the fixed point $x = (0,0)$ we have

$$E(0,0) = 0; \quad DE(0,0) = 0 \in \mathbb{R}^{2\times 2}; \quad D^2E(0,0) = \begin{pmatrix} mgl & 0 \\ 0 & ml^2 \end{pmatrix}.$$

We have that the Hessian of E is positive definite. Therefore E is positive definite at $(0,0)$. Further we have

$$\dot{E}(x) = \langle DE(x), f(x)\rangle = \begin{pmatrix} mgl\sin(x_1) & ml^2x_2 \end{pmatrix} \begin{pmatrix} x_2 \\ -\frac{g}{l}\sin(x_1) \end{pmatrix} = 0.$$

Thus $\dot{E}$ is negative semidefinite. Now the hypotheses of Theorem 3.14 are fulfilled, hence $x = (0,0)$ is Lyapunov stable. Importantly, this is a nonlinear result and we did not need to refer to the linearization of the system!

At the fixed point $x = (\pi, 0)$. We check again using the energy. First we realize that $E(\pi,0) = 2mgl$, so we subtract the constant and redefine to obtain $\tilde{E} = E - 2mgl$. Now $\tilde{E}(\pi,0) = 0$, although this is not essential. Next we calculate

$$DE(\pi,0) = 0 \in \mathbb{R}^{n\times n}; \quad D^2E(\pi,0) = \begin{pmatrix} -mgl & 0 \\ 0 & ml^2 \end{pmatrix}.$$

Hence, E is indefinite at $(\pi,0)$. From the previous calcuation we alread know that $\dot{E}(\pi,0) = 0$, i.e. $\dot{E}$ is semidefinite. We cannot apply Theorem 4, but linearization already concluded that $(\pi,0)$ was unstable.

Example 3.13 (Stability analysis of the friction pendulum). We have a shaft which is constantly rotating with angular speed Ω, around this shaft is a sleeve which rubs against the shaft creating friction. To this sleeve is a mass m attached at distance l, the deflection of this mass from its standard position (directly below the shaft) is measured by φ. The gravity constant is given by g. This setup is depicted in Fig. 3.25. The torque driving the pendulum is given by

$$T(\dot{\varphi}) = T_0\mathrm{sign}(\Omega - \dot{\varphi}).$$

From this we get the equation of motion

$$ml^2\ddot{\varphi} + mgl\sin(\varphi) = T(\dot{\varphi}) = T_0\mathrm{sign}(\Omega - \dot{\varphi}).$$

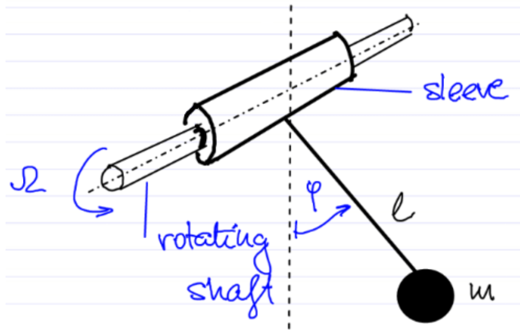

Figure 3.25: The setup of the friction pendulum.

By assuming $\Omega \gg 1$, i.e. very fast rotation of the shaft, we find that $T(\dot{\varphi}) = T_0$. Next we transform the coordinates in order to get an ODE

$$\begin{pmatrix} x_1 \\ x_2 \end{pmatrix} = \begin{pmatrix} \varphi \\ \dot{\varphi} \end{pmatrix}; \quad \begin{pmatrix} \dot{x}_1 \\ \dot{x}_2 \end{pmatrix} = \begin{pmatrix} x_2 \\ -\frac{g}{l}\sin(x_1) + \frac{T_0}{ml^2} \end{pmatrix}.$$

Thus the fixed point x_0 is at $(\overline{x}_1, \overline{x}_2)$ given by

$$\sin(\overline{x}_1) = \frac{T_0}{mgl}; \quad \overline{x}_2 = 0.$$

Since the system is forced, energy is not conserved and we cannot use it as a Lyapunov function. However, there may still exist a conserved quantity. Consider using

$V(x) = $ [total energy at time t] $-$ [work put in between time t and t_0] $=$ [initial energy] $=$ const.

This is a conserved quantity in all mechanics problems, but generally cannot be calculated without already knowing the trajectories. Here we can, as

$$V(x(t)) = \frac{1}{2}mlx_0^2 + mgl(1 - \cos(x_1)) - T_0(\underbrace{x_1}_{\varphi(t)} - \underbrace{x_1(0)}_{\varphi(0)}).$$

We can drop the constant term $T_0 x_1(0)$. Now verify that V is indeed constant

$$\dot{V}(x) = \frac{\partial V}{\partial x_1}\dot{x}_1 + \frac{\partial V}{\partial x_2}\dot{x}_2 = (mgl\sin(x_1) - T_0)\, x_2 + ml^2 x_2 \left(-\frac{g}{l}\sin(x_1) + \frac{T_0}{ml^2}\right) = 0.$$

Hence $\dot{V}(x)$ is semidefinite, and may be used to conclude stability or instability. We must check the Lyapunov conditions for $V(x)$

$$DV(x_0) = \begin{pmatrix} mgl\sin(\overline{x}_1) - T_0 & ml^2\overline{x}_2 \end{pmatrix} = \begin{pmatrix} 0 & 0 \end{pmatrix}$$
$$D^2V(x_0) = \begin{pmatrix} mgl\cos(\overline{x}_1) & 0 \\ 0 & ml^2 \end{pmatrix}.$$

The Hessian is positive definite as long as $\overline{x}_1 \in \left(-\frac{\pi}{2}, \frac{\pi}{2}\right)$, and all fixed points in this region are stable by Theorem 3.14. The Hessian is indefinite if $\overline{x}_1 \notin \left[-\frac{\pi}{2}, \frac{\pi}{2}\right]$, but in this case Theorem 4 is not applicable as $\dot{V}$ is not definite.

Chapter 4

Bifurcations of fixed points

4.1 Local nonlinear dynamics near fixed points

We are interested in the local nonlinear dynamics around fixed points. Consider

$$\dot{x} = f(x); \quad f \in C^r, r \geq 1; \quad f(p) = 0, \tag{4.1}$$

i.e. p is a fixed point of the dynamical system. The linearized system at p is

$$\dot{y} = Df(p)y, \ y \in \mathbb{R}^n, \ Df(p) \in \mathbb{R}^{n\times n}. \tag{4.2}$$

The linearization has the eigenvalues $\lambda_1, \dots, \lambda_n \in \mathbb{C}$ with multiplicities counted. Corresponding to these eigenvalues are the eigenvectors $e_1, \dots, e_n \in \mathbb{C}^n$, including generalized eigenvectors for when the algebraic multiplicity is greater than the geometric multiplicity. The eigenvector e_j is real when $\lambda_j \in \mathbb{R}$.

Definition 4.1. The following subspaces are invariant for the linearized dynamical system:

(i) The *stable subspace*

$$\boxed{E^S = \operatorname{span}_j \{\operatorname{Re}(e_j), \operatorname{Im}(e_j) : \ \operatorname{Re}(e_j) < 0\},}$$

(ii) The *unstable subspace*

$$\boxed{E^U = \operatorname{span}_j \{\operatorname{Re}(e_j), \operatorname{Im}(e_j) : \ \operatorname{Re}(e_j) > 0\},}$$

(iii) The *center subspace*

$$\boxed{E^C = \operatorname{span}_j \{\operatorname{Re}(e_j), \operatorname{Im}(e_j) : \ \operatorname{Re}(e_j) = 0\}.}$$

Remark 4.1. Note here that the following facts hold

(i) $E^C = \emptyset$ if and only if p is hyperbolic,

(ii) $E^{U,S}$ and E^C are invariant subspaces of (4.2) by construction,

(iii) Solutions of (4.2) in E^S (resp. E^U) decay to $y = 0$ as $t \to \infty$ (resp. $t \to -\infty$).

We now ask ourselves what happens to these subspaces in the nonlinear system.

Theorem 4.2 (Center Manifold Theorem)**.** *The following hold:*

(i) There exists a unique stable manifold $W^S(p)$ *for* (4.1)*, such that*

- $W^S(p)$ *is a* C^r *manifold (surface), tangent to* E^S *at* p *with* $dim W^S(p) = dim E^S$*,*
- $W^S(p)$ *is invariant for* (4.1) *and for* $x \in W^S(p)$ *we have*

$$\|F^t(x)\| \leq K_S \exp\left[t\left(\max_{Re(\lambda_j)<0}(Re(\lambda_j)) + \epsilon_S\right)\right]$$

for $t \geq 0$, $0 < \epsilon_S \ll 1$, *and* $\|x - p\|$ *small enough.*

(ii) There exists a unique unstable manifold $W^U(p)$ *for* (4.1)*, such that*

- $W^U(p)$ *is a* C^r *manifold (surface), tangent to* E^U *at* p *with* $dim W^U(p) = dim E^U$*,*
- $W^U(p)$ *is invariant for* (4.1) *and for* $x \in W^U(p)$ *we have*

$$\|F^t(x)\| \leq K_U \exp\left[t\left(\max_{Re(\lambda_j)>0}(Re(\lambda_j)) + \epsilon_U\right)\right]$$

for $t \geq 0$, $0 < \epsilon_U \ll 1$, *and* $\|x - p\|$ *small enough.*

(iii) There exists a (not necessarily unique) center manifold $W^C(p)$ *for* (4.1)*, such that*

- $W^C(p)$ *is a* C^{r-1} *manifold (surface), tangent to* E^C *at* p *with* $dim W^C(p) = dim E^C$*,*

The geometry of these manifolds is sketched in Fig. 4.1.

The overall dynamics depend crucially on the center manifold, especially when $E^U = \emptyset$, i.e. the stability type is determined by $W^C(p)$. Hence why it will be the subject of our further investigation.

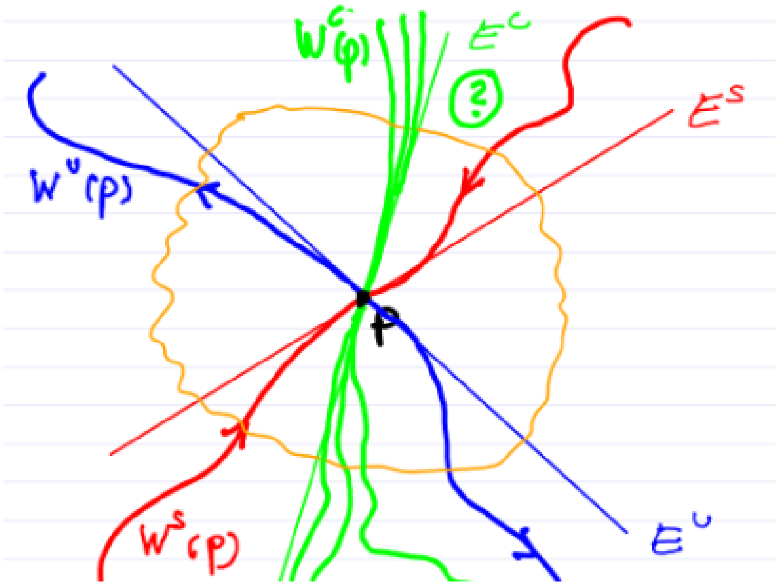

Figure 4.1: A sketch of the stable (red), unstable (blue), and center manifolds (green), along with their respective invariant linear subspaces. Note the existence of multiple center manifolds and the singular unique unstable/stable manifolds.

4.2 The center manifold

Example 4.1 (Uniqueness of the center manifold). We would like to explore if the center manifold is generally non-unique. Consider the dynamical system

$$\begin{cases} \dot{x} = x^2 \\ \dot{y} = -y. \end{cases}$$

First, linearize at the origin to find the linearized dynamics

$$A = Df(0) = \begin{pmatrix} 0 & 0 \\ 0 & -1 \end{pmatrix}.$$

These linearized dynamics are illustrated in Fig. 4.2. We find the invariant subspaces

$$E^C = \text{span}\left\{\begin{pmatrix} 1 \\ 0 \end{pmatrix}\right\}; \quad E^S = \text{span}\left\{\begin{pmatrix} 0 \\ 1 \end{pmatrix}\right\}; \quad E^U = \emptyset.$$

The nonlinear manifolds are illustrated with the invariant subspaces from the linearization in Fig. 4.2. Observe there exist infinitely many center manifolds which are all invariant and all tangent to E^C at the origin. We also see that although the fixed point at the origin is stable in the linearized system, it is unstable in the nonlinear system.

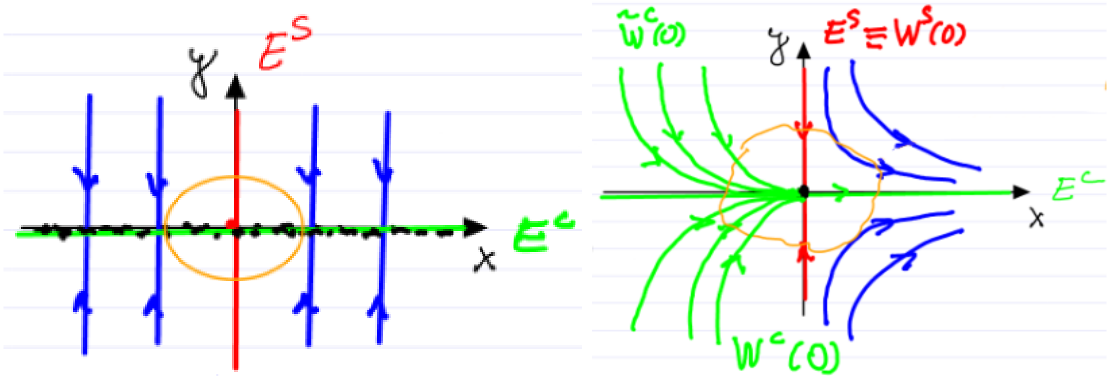

Figure 4.2: Left: The linearized dynamics around the origin. Right: The nonlinear phase portrait.

We are left with the question: how can we calculate $W^C(p)$ in general?

(i) Consider

$$\dot{z} = F(z); \quad F(0) = 0; \quad z \in \mathbb{R}^{c+d}; \quad F \in C^r.$$

Where c represents the number of center directions at the origin ($\dim E^C$) and d denoted the remaining directions ($\dim E^U + \dim E^S$).

(ii) Now block-diagonalize the linearization. This consists of four steps

(a) First linearize the dynamics to find $\dot{z} = Mz + \mathcal{O}(\|z\|^2)$ with $M = DF(0) \in \mathbb{R}^{(c+d)\times(c+d)}$.

(b) Define the transformation matrix

$$T = \begin{bmatrix} a_1 & \dots & a_c & b_1 & \dots & b_d \end{bmatrix} = \begin{bmatrix} \text{basis in } E^C & \text{basis in } E^U \oplus E^S \end{bmatrix}.$$

(c) Pass to the basis from the transformation matrix with $z = T\xi$

$$\dot{\xi} = T^{-1}\dot{z} = T^{-1}MT\xi + T^{-1}\mathcal{O}(\|T\xi\|^2) = \begin{pmatrix} A & 0 \\ 0 & B \end{pmatrix} \xi + \mathcal{O}(\|\xi\|^2).$$

The matrices A and B are elements of $\mathbb{R}^{c\times c}$ and $\mathbb{R}^{d\times d}$ respectively.

(d) Let $\xi = \begin{pmatrix} x \\ y \end{pmatrix} \in \mathbb{R}^c \times \mathbb{R}^d$, the x-coordinates is aligned with E^C and the y-coordinates are perpendicular. We then find

$$\dot{x} = Ax + f(x, y); \quad \dot{y} = By + g(x, y),$$

for $f, g \in C^r$ and $f, g = \mathcal{O}(\|x\|^2, \|y\|^2, \|x\|\|y\|)$. The geometry in these coordinates is depicted in Fig. 4.3. The center manifold is given by

$$W^C(0) = \{(x, y) \in U : \; y = h(x)\}$$

for $h : \mathbb{R}^c \to \mathbb{R}^d$ and $h \in C^{r-1}$ as in the theorem.

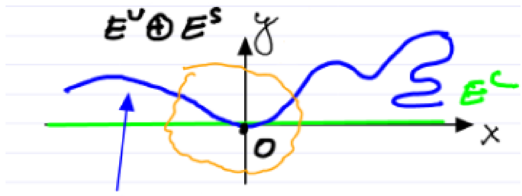

Figure 4.3: The geometry of the nonlinear system in the transformed coordinates aligned with the invariant subspaces of the linearization. The blue arrow points to the center manifold $W^C(0)$.

(iii) Now we use the invariance of $W^C(0)$, i.e. for all t it holds $y(t) = h(x(t))$ to find

$$\dot{y} = Dh(x(t))\dot{x}(t),$$

which implies the nonlinear partial differential equation (PDE) for $h(x)$

$$\boxed{Bh(x) + g(x, h(x)) = Dh(x)\,[Ax + f(x, h(x))]\,.} \tag{4.3}$$

We cannot solve this analytically.

(iv) Instead take the Taylor expansion of (4.3) to approximate the solution

$$h(x) = \underbrace{h(0)}_{=0} + \underbrace{Dh(0)}_{=0}\,x + \frac{1}{2}\underbrace{D^2h(0)}_{3-\text{tensor}} \otimes x \otimes x + \mathcal{O}(\|x\|^3),$$

where the first two terms are 0 due to the tangency to E^C at 0. We therefore have that $h(x) = \mathcal{O}(\|x\|^2)$. Therefore we seek $W^C(0)$ of this form. We get the dynamics on the center manifolds

$$\boxed{\dot{x} = Ax + f(x, h(x)).}$$

Example 4.2 (Finding the center manifold). Consider the dynamical system

$$\begin{cases} \dot{x} = xy \\ \dot{y} = -y + \alpha x. \end{cases}$$

First we linearize at $(0,0)$ to get

$$M = \begin{pmatrix} [0] & [0] \\ [0] & [-1] \end{pmatrix}$$

which is already in block-matrix form. The dimensions of the stable, unstable, and center subspaces of the linearization are 1, 0, and 1 respectively. Hence the stability type depends on the dynamics on the center manifold $W^C(0)$. We now look for an equation to parameterize $W^C(0)$

$$h(x) = ax^2 + bx^3 + cx^4 + \mathcal{O}(x^5).$$

This is a finite expansion and thus in general will not converge as that would imply the center manifold is unique. Now use the invariance (the PDE we already derived) to find

$$\dot{y} = h'(x)\dot{x} = \left[2ax + 3bx^2 + 4cx^3 + \mathcal{O}(x^4)\right] x \left[ax^2 + bx^3 + cx^4 + \mathcal{O}(x^5)\right]. \tag{4.4}$$

On the other hand, from the dynamical system we know

$$\dot{y} = -h(x) + \alpha x^2 = (\alpha - a)x^2 - bx^3 - cx^4 + \mathcal{O}(x^5). \tag{4.5}$$

Comparing coefficients of equal powers in (4.4) and (4.5).

$$\begin{aligned} \mathcal{O}(x^2) &: \ \alpha = a \\ \mathcal{O}(x^3) &: \ b = 0 \\ \mathcal{O}(x^4) &: \ 2a^2 = -c. \end{aligned}$$

Therefore we find

$$\boxed{h(x) = \alpha x^2 - 2\alpha^2 x^4 + \mathcal{O}(x^5).}$$

Then the dynamics on $W^C(0)$ become

$$\boxed{\dot{x} = xh(x) = \alpha x^3(1 - 2\alpha x^2) + \mathcal{O}(x^6).}$$

These dynamics are depicted in Fig. 4.4. For $\alpha > 0$ the origin is unstable, meanwhile for $\alpha < 0$ the origin is asymptotically stable.

The full local stable manifold for $\alpha < 0$ is $\overline{W}^S(0) = U$ and it is of dimension 2. The difference between $\overline{W}^S(0)$ and $W^S(0)$ is that in general the decay rate is generally weaker than the rate guaranteed in the Center Manifold Theorem.

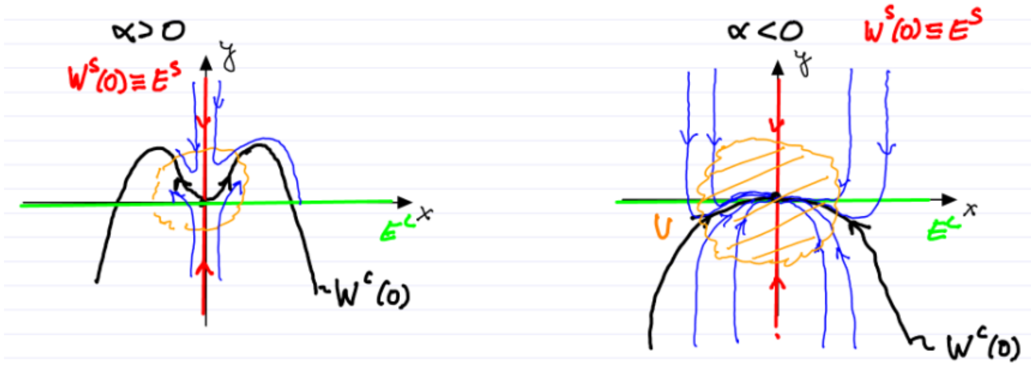

Figure 4.4: Left: The nonlinear dynamics on the center manifold for $\alpha > 0$. Right: The nonlinear dynamics on the center manifold for $\alpha < 0$.

Remark 4.3. The $\mathcal{O}(x^5)$ truncation has two hyperbolic fixed points at $x = \pm\frac{1}{\sqrt{2\alpha}}$, however the full system has no such fixed points. The reason for this is that away from the origin, the $\mathcal{O}(x^6)$ terms are no longer guaranteed to be small relative to the $\mathcal{O}(x^5)$ terms, and the truncation this far away from 0 is not justified.

After this example we would like to explore if the concept of the center manifold is robust, as the existence of eigenvalues with $\mathrm{Re}(\lambda_i) = 0$ is not. We will explore this in an example.

Example 4.3 (Perturbing the previous example). Consider the following perturbed dynamical system

$$\begin{cases} \dot{x} = xy + \epsilon x \\ \dot{y} = -y + \alpha x^2 \end{cases}; \quad |\epsilon| \ll 1.$$

The linearization of this system yields

$$\begin{cases} \dot{x} = \varepsilon x \\ \dot{y} = -y. \end{cases}$$

I used varepsilon instead of epsilon here, I like that and think we should use it everywhere.
Now the center manifold disappears as the center subspace E^C disappears for $\epsilon > 0$!

4.3 Center manifolds depending on parameters

We begin with the setup

$$\begin{cases} \dot{x} = Ax + f(x, y, \epsilon) \\ \dot{y} = By + g(x, y, \epsilon) \end{cases}; \quad x \in \mathbb{R}^c,\ y \in \mathbb{R}^d,\ 0 \le \epsilon \ll 1;$$
$$f, g \in C^r,\ f, g = \mathcal{O}(\|x\|^2, \|y\|^2, \|x\|\|x\|, \epsilon\|x\|, \epsilon\|y\|).$$

The order $\epsilon\|x\|$ and $\epsilon\|y\|$ terms are due to the perturbation of the linear part. Now assume $\mathrm{Re}(\lambda_j(A)) =$ for $j = 1, \dots, c$ (the center directions) and $\mathrm{Re}(\lambda_j(B)) \neq$ for $j = 1, \dots,$ (the hyperbolic directions). Next, rewrite $\tilde{x} = \begin{pmatrix} x \\ \epsilon \end{pmatrix}$ and $\tilde{y} = y$ to obtain the system

$$\begin{cases} \dot{\tilde{x}} = \tilde{A}\tilde{x} + \tilde{f}(\tilde{x}, \tilde{y}) \\ \dot{\tilde{y}} = \tilde{B}\tilde{y} + \tilde{g}(\tilde{x}, \tilde{y}) \end{cases}; \quad \tilde{A} = \begin{pmatrix} A & 0 \\ 0 & 0 \end{pmatrix} \in \mathbb{R}^{(c+1)\times(c+1)}; \quad \tilde{f} = \begin{pmatrix} f \\ 0 \end{pmatrix}. \tag{4.7}$$

Here, $\tilde{g} = g$ and $\tilde{B} = B$. Further, note that span $\left\{ \begin{pmatrix} x \\ 0 \end{pmatrix} \right\}$ is an invariant subspace for $\tilde{A}$. The eigenvalues of $\tilde{A}$ are the same as those of A and an additional 0, thus there are $c + 1$ center directions and d hyperbolic directions. Applying the center manifold theorem to the fixed point $0 \in \mathbb{R}^{c+1+d}$ of (4.7) we obtain that there exists a $\tilde{W}^C(0)$ C^{r-1} manifold tangent to E^C at $\begin{pmatrix} \tilde{x} \\ \tilde{y} \end{pmatrix} = \begin{pmatrix} 0 \\ 0 \end{pmatrix}$ which is invariant and is dimension $c+1$. The geometry of this manifold is illustrated in Fig. 4.5. Note in the figure that there is no dynamics in the ϵ direction, as $\dot{\epsilon} = 0$ and that $(x, y) = (0, 0) \in \mathbb{R}^{c+d}$ remains a fixed point for $\epsilon \neq 0$.

Computing $\tilde{W}^C(0)$ is done in a similar fashion as before. We use the center manifold theorem to get

$$\tilde{y} = y = \tilde{h}(\tilde{x}) = \tilde{h}(x, \epsilon) = \mathcal{O}(\|x\|^2, \epsilon\|x\|, \epsilon^2) = \mathcal{O}(\|x\|^2, \epsilon\|x\|).$$

The order ϵ^2 term was dropped as $x = 0$ must remain a fixed point. The function h describes the graph of $W^C_\epsilon(0)$. Then the reduced dynamics on $W^C_\epsilon(0)$ are

$$\boxed{\dot{x} = Ax + f(x, \tilde{h}(x, \epsilon), \epsilon).}$$

This can then be applied to the perturbed example from above.

Example 4.4 (Revisting the perturbation). Recall the dynamical system

$$\begin{cases} \dot{x} = xy + \epsilon x \\ \dot{y} = -y + \alpha x^2. \end{cases}$$

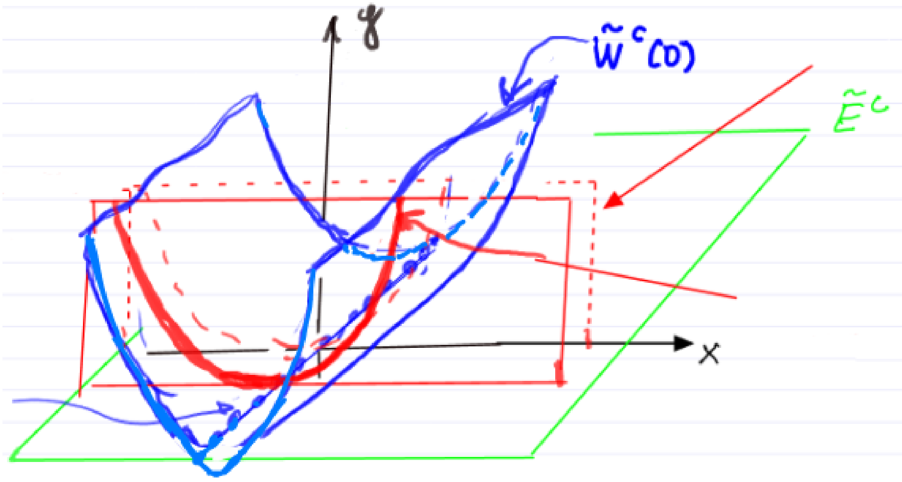

Figure 4.5: Geometry of the center manifold with the perturbation. The straight red arrow designates the cut at $\epsilon = 0$ which is equal to $W^C(0)$, the squiggly red arrow points at the continuation of the center manifold from $\epsilon = 0$ to $\epsilon \neq 0$.

We have the persisting fixed point at $(x, y) = (0, 0) \in \mathbb{R}^{c+d}$ and the system is already in standard form with

$$A = 0; \quad B = -1; \quad f(x, y, \epsilon) = xy + \epsilon x; \quad g(x, y, \epsilon) = -\alpha x^2.$$

We apply the center manifold theorem and get the existence of $W^C_\epsilon(0)$ for $|\epsilon| \ll 1$. This manifold satisfies

$$y = \tilde{h}(x, \epsilon) = ax^2 + bx\epsilon + c\epsilon^2 + dx^3 + ex^2\epsilon + jx\epsilon^2 + k\epsilon^3 + kx^4 \dots . \tag{4.8}$$

The term $c\epsilon^2$ must be equal to 0 for all ϵ such that the fixed point persists, therefore $c = 0$. Next the invariance $y(t) = \tilde{h}(x(t)), \epsilon)$ is used, taking the time derivative on both sides yields

$$\dot{y} = [2ax + b\epsilon + \mathcal{O}(2)] \quad \underbrace{[\mathcal{O}(3) + \epsilon x]}_{=\dot{x} \text{ from ODE and (4.8)}} \quad = 2a\epsilon x^2 + b\epsilon^2 x + \mathcal{O}(4).$$

The $\mathcal{O}(n)$ designates terms of total degree n, for example x^n or $x^{n-k}\epsilon^k$. From the ODE we find

$$\dot{y} = -y + \alpha x^2 = -ax^2 - bx\epsilon - c\epsilon^2 - dx^3 - ex^2\epsilon - jx\epsilon^2 - k\epsilon^3 - \mathcal{O}(4) + \alpha x^2.$$

Comparing equal powers in these two equations we find

$$\mathcal{O}(x^2): \; 0 = \alpha - a; \qquad \mathcal{O}(\epsilon^2): \; 0 = -c; \qquad \mathcal{O}(x\epsilon): \; 0 = -b;$$
$$\mathcal{O}(\epsilon^3): \; 0 = -t; \qquad \mathcal{O}(x^3): \; 0 = -d; \qquad \mathcal{O}(x^2\epsilon): \; 2a = -e;$$
$$\mathcal{O}(x\epsilon^2): \; b = -j.$$

Thus the shape of $W_\epsilon^C(0)$ is given by

$$y = \tilde{h}(x, \epsilon) = \alpha(1 - 2\epsilon)x^2 + \mathcal{O}(4).$$

The dynamics on $W_\epsilon^C(0)$ are

$$\dot{x} = \epsilon x + \alpha(1 - 2\epsilon)x^3 + \mathcal{O}(5).$$

We can see there is no substantial change in the shape of $W_\epsilon^C(0)$ relative to the $\epsilon = 0$ case. The stability type is determined by the sign of ϵ and a two time-scale dynamic persists.

From this example we may still wonder what the effect of the higher order terms have for an effect of the center manifold.

4.4 Normal forms

For a general treatment see the book by Guckenheimer & Holmes, here we will consider one example to illustrate the idea (Poincare).

Example 4.5 (Reduced dynamics on 1-dimensional manifold). Consider the following 1-dimensional dynamical system

$$\dot{x} = x(\mu - x^2) + x^4; \quad 0 \leq |\mu| \ll 1.$$

The fixed points are at $x = 0$ and the roots of $g_\mu(x) = \mu - x^2 + x^3$. This function g_μ is illustrated in Fig. 4.6. By plotting x as a function of μ such that $g_\mu(x)$ we get the *bifurcation diagram* as

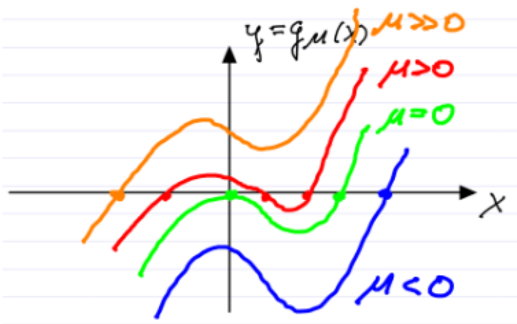

Figure 4.6: The functions g_μ for different values of μ.

shown in Fig. 4.7.

The fold bifurcation (see caption of Fig. 4.7) is created by quartic (order 4) terms, which become more important away from the origin. The pitchfork bifurcation is already captured by

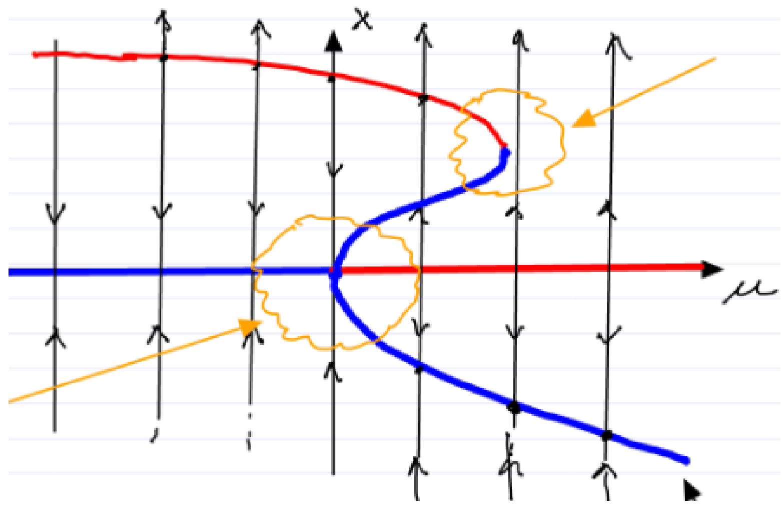

Figure 4.7: Bifurcation diagram for the 1-dimensional dynamical system. Red and blue demarcate if the fixed point at the given (x, μ) pair is stable (blue) or unstable (right). The arrow on the right points towards a *fold bifurcation* and the arrow on the left towards a *pitchfork bifurcation*.The curve is given by implicitly solving $g_\mu(x) = 0$.

the cubic truncation. We would like to know when the truncation captures the full dynamics correctly near the origin. Poincare showed that, in fact, the truncated system is topologically equivalent to the full system near the origin by using a change of coordinates to remove $\mathcal{O}(4)$ terms.

(i) Let $x = y + h_4(y) = y + ay^4 + \mathcal{O}(y^5)$, which is near the identity near the origin, hence it is also invertible near the origin (by Implicit Function Theorem). Further, this preserves the ODE up to the $\mathcal{O}(3)$ terms.

(ii) Plug in $x(t)$ and $y(t)$ and take the derivative with respect to time to get

$$\dot{x} = \dot{y}(1 + 4ay^3 + \mathcal{O}(y^4)).$$

(iii) Now use the ODE and find

$$\dot{x} = \mu x - x^3 + x^4 = \mu(y + ay^4) - (y + ay^4)^3 + (y - ay^4)^5 + \dots .$$

(iv) Combine the previous two steps and calculate

$$\dot{y} = \left[1 + 4ay^3 + \mathcal{O}(y^4)\right]^{-1}\left[\mu y + a\mu y^4 - y^3 + y^4 + \mathcal{O}(5)\right].$$

At this point recall the von Neumann series (verify with Taylor expansion)

$$\frac{1}{1+z} = 1 - z + \mathcal{O}(z^2); \quad 0 \leq |z| \ll 1.$$

Applying this to the left term in the formula for $\dot{y}$ yields

$$\left[1 + 4ay^3 + \mathcal{O}(y^4)\right]^{-1} = 1 - 4ay^3 + \mathcal{O}(y^4).$$

Therefore we find

$$\dot{y} = \mu y - y^3 + y^4 \underbrace{(-4a\mu + a\mu + 1)}_{\text{choose } a \text{ such that this } =0} + \mathcal{O}(y^5),$$

the a that fulfills this is $a = \frac{1}{3\mu}$, using this we find

$$\boxed{\dot{y} = \mu y - y^3 + \mathcal{O}(y^5).}$$

This transformation has removed the quartic terms from the equation.

(v) Now we remove the $\mathcal{O}(y^5)$ terms similarly. First set

$$y = \xi + h_5(\xi) = \xi + b\xi^5 + \mathcal{O}(\xi^6)$$

and then continue as before, but with y now playing the role of x and ξ playing the role of y.

(vi) The successive sequence of near identity coordinate changes turns out to converge usually. In general, it depends on the type of problem, sometimes resonant terms are not removeable and must stay as they are crucial to the dynamics. These terms depend on the linear part, for more see the book by Guckenheimer & Holmes.

Thus

$$\boxed{\dot{x} = \mu x - x^3}$$

is the *normal form* for the ODE for the study of bifurcations at the origin for $0 \leq \mu \ll 1$. It is topologically equivalent to the full system near $x = 0$ and captures the pitchfork bifurcation.

4.5 Bifurcations

A *bifurcation* is a qualitative change in the dynamical system

$$\boxed{\dot{x} = f(x, \mu); \quad x \in \mathbb{R}^n; \quad \mu \in \mathbb{R}^p.} \tag{4.9}$$

Linear stability analysis led to reducing to the center manifold (depending on parameters). From there we moved to normal forms which enable the analysis of qualitative dynamics under varying parameters.

Definition 4.2 (Local bifurcation)**.** A *local bifurcation* is a local near-equilibrium change in qualitative behavior. More precisely, a *bifurcation* occurs in (4.9) at $\mu = \mu_0$ near the fixed point $x = 0$ if there exists no neighborhood of $x = 0$ in which $\dot{x} = f(x, \mu_0)$ is topologically equivalent to <u>all</u> systems $\dot{x} = f(x, \mu)$ for $\|\mu - \mu_0\|$ small enough.

This idea of a bifurcation can be illustrated by a "bifurcation" surface which separates the space of dynamical systems into components. Within each component the dynamical systems are topologically equivalent, however elements from separate components are not. This is sketched in Fig. 4.8.

Figure 4.8: Illustration of a bifurcation surface (blue). The near side of the surface is one component, and the far side the other. The red path is a family of dynamical systems $\{\dot{x} = f(x, \mu)\}_{\mu \in \mathbb{R}^p}$, going through the bifurcation point μ_0. Around this point, a neighborhood as outlined in the definition is sketched in orange.

We wish to understand what happens in the case that a given family of dynamical systems is nongeneric (atypical). For instance in the case that the family forms a tangency to the bifurcation surface, in which case a bifurcation does not take place, hence the family of dynamical systems is not general enough to capture all possible dynamics.

Example 4.6 (Nongeneric family of dynamical systems). In comparison to the family taken previously consider

$$\dot{x} = -a^2 x - x^3; \quad \mu = -a^2 \leq 0.$$

For every μ which we consider, there is only one fixed point $x = 0$ and it is stable for all values of μ. However, we have unwittingly missed the full picture, as for $\mu > 0$ there are three fixed points, two of which are unstable. This situation is shown in Fig. 4.9.

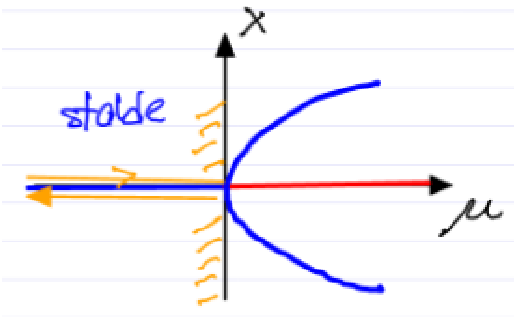

Figure 4.9: A nongeneric family of dynamical systems. We only see what happens to the left of the x-axis, and miss everything to the right, hence our family is tangent to the bifurcation surface.

This idea of nongeneric families leads us to our next definition which is also depicted in Fig. 4.10.

Definition 4.3 (Universal unfolding)**.** A paramaterized family of dynamical systems crossing all nearby topological equivalence classes as the parameters vary is called a *universal unfolding.*

Definition 4.4 (Codimension of a bifurcation)**.** The *codimension of a bifurcation* is the minimum number of parameters required for a universal unfolding. Thus a more degenerate bifurcation requires a larger codimension.

4.6 Codimension 1 bifurcations

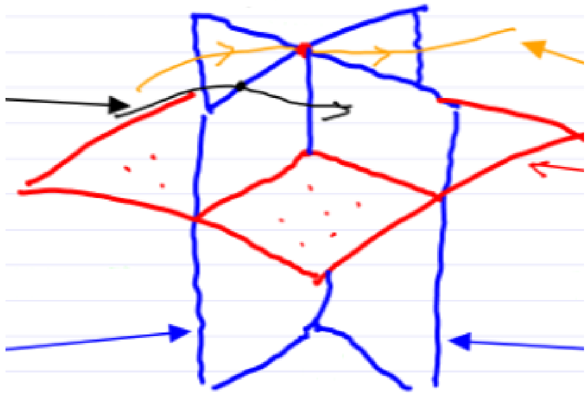

Figure 4.10: An example of universal unfolding (red) for the red bifurcation point which crosses the four topologically equivalent classes (components) created by the two bifurcation surfaces (blue). Furthermore, a nonuniversal unfolding is shown by the yellow 1-dimensional path at the top. Another universal unfolding in for the black bifurcation point, is shown by the 1-dimensional black family.